

# Genetically Encoded Biosensors Reveal PKA Hyperphosphorylation on the Myofilaments in Rabbit Heart Failure

Federica Barbagallo,\* Bing Xu,\* Gopireddy R. Reddy, Toni West, Qingtong Wang, Qin Fu, Minghui Li, Qian Shi, Kenneth S. Ginsburg, William Ferrier, Andrea M. Isidori, Fabio Naro, Hemal H. Patel, Julie Bossuyt, Donald Bers, Yang K. Xiang

**Rationale:** In heart failure, myofilament proteins display abnormal phosphorylation, which contributes to contractile dysfunction. The mechanisms underlying the dysregulation of protein phosphorylation on myofilaments is not clear.

**Objective:** This study aims to understand the mechanisms underlying altered phosphorylation of myofilament proteins in heart failure.

**Methods and Results:** We generate a novel genetically encoded protein kinase A (PKA) biosensor anchored onto the myofilaments in rabbit cardiac myocytes to examine PKA activity at the myofilaments in responses to adrenergic stimulation. We show that PKA activity is shifted from the sarcolemma to the myofilaments in hypertrophic failing rabbit myocytes. In particular, the increased PKA activity on the myofilaments is because of an enhanced  $\beta_2$  adrenergic receptor signal selectively directed to the myofilaments together with a reduced phosphodiesterase activity associated with the myofibrils. Mechanistically, the enhanced PKA activity on the myofilaments is associated with downregulation of caveolin-3 in the hypertrophic failing rabbit myocytes. Reintroduction of caveolin-3 in the failing myocytes is able to normalize the distribution of  $\beta_2$  adrenergic receptor signal by preventing PKA signal access to the myofilaments and to restore contractile response to adrenergic stimulation.

**Conclusions:** In hypertrophic rabbit myocytes, selectively enhanced  $\beta_2$  adrenergic receptor signaling toward the myofilaments contributes to elevated PKA activity and PKA phosphorylation of myofilament proteins. Reintroduction of caveolin-3 is able to confine  $\beta_2$  adrenergic receptor signaling and restore myocyte contractility in response to  $\beta$  adrenergic stimulation. (*Circ Res.* 2016;119:931-943. DOI: 10.1161/CIRCRESAHA.116.308964.)

**Key Words:** adrenergic receptor ■ heart failure ■ myofibrils ■ phosphorylation ■ protein kinase A

In animal hearts, elevated sympathetic activity stimulates the  $\beta$ -adrenergic signal to promote inotropy and lusitropy via the concerted protein kinase A (PKA) phosphorylation of substrates at multiple subcellular locations. PKA is spatially and temporally regulated through a set of A-kinase anchoring protein complexes.<sup>1</sup> As a result, the precise PKA phosphorylation of myofilament proteins, such as cardiac troponin I (TnI) and myosin-binding protein C, and  $\text{Ca}^{2+}$ -handling proteins, such as phospholamban (PLB) and ryanodine receptor on the sarcoplasmic reticulum (SR), is necessary to co-ordinate positive inotropic and lusitropic cardiac effects.<sup>2,3</sup>

Chronic adrenergic signaling also promotes structural and functional remodeling in the myocardium, which contributes to cardiac hypertrophy and eventually heart failure in a variety of clinical conditions. A desensitized cardiac  $\beta$  adrenergic receptor ( $\beta$ AR) signaling pathway,<sup>4</sup> a hallmark of the failing heart, is associated with a reduced number of  $\beta_1$ AR- but not  $\beta_2$ AR-binding sites at the plasma membrane (PM). As a consequence, diminished  $\beta$ AR signaling may lead to lower PKA-mediated protein phosphorylation after adrenergic stimulation.<sup>5</sup> The disturbed  $\beta$ AR signaling and reduced PKA phosphorylation result in blunted contractile response after administration of  $\beta$ AR agonists.<sup>6</sup> Interestingly, recent

Original received April 23, 2016; revision received August 26, 2016; accepted August 29, 2016. In July 2016, the average time from submission to first decision for all original research papers submitted to *Circulation Research* was 13.27 days.

From the Department of Pharmacology, University of California at Davis (F.B., B.X., G.R.R., T.W., Q.W., Q.F., M.L., Q.S., K.S.G., J.B., D.B., Y.K.X.); Department of Experimental Medicine (F.B., A.M.I.) and Department of Anatomical, Histological, Forensic, and Orthopedic Sciences (F.N.), Sapienza University of Rome, Italy; Department of Medicine and Epidemiology, School of Veterinary Medicine, and Surgical Research Facility, School of Medicine, University of California, Davis (W.F.); VA San Diego Healthcare System, La Jolla, CA (H.H.P.); Department of Anesthesiology, University of California, San Diego, La Jolla (H.H.P.); and VA Northern California Healthcare System, Mather (Y.K.X.).

\*These authors contributed equally to this article.

The online-only Data Supplement is available with this article at <http://circres.ahajournals.org/lookup/suppl/doi:10.1161/CIRCRESAHA.116.308964/-DC1>.

Correspondence to Dr Yang K. Xiang, Department of Pharmacology, University of California at Davis, Davis, CA 95616. E-mail [ykxiang@ucdavis.edu](mailto:ykxiang@ucdavis.edu)  
© 2016 American Heart Association, Inc.

*Circulation Research* is available at <http://circres.ahajournals.org>

DOI: 10.1161/CIRCRESAHA.116.308964

**Nonstandard Abbreviations and Acronyms**

<b>AKAR</b>	A-kinase activity reporter
<b>βAR</b>	β adrenergic receptor
<b>C3SD</b>	scaffolding domain of caveolin-3
<b>FRET</b>	fluorescence resonant energy transfer
<b>HF</b>	heart failure
<b>ISO</b>	isoproterenol
<b>PDE</b>	phosphodiesterase
<b>PKA</b>	protein kinase A
<b>PLB</b>	phospholamban
<b>PM</b>	plasma membrane
<b>SR</b>	sarcoplasmic reticulum
<b>TnI</b>	troponin I

progress suggests that βAR can continuously signal both at the cell surface<sup>7</sup> and after catecholamine-induced endocytosis.<sup>8</sup> These βAR signals may play a role in adaptive cardiac hypertrophic remodeling and promote compensatory contractility in the heart. Until now, it remains poorly understood how remodeling of βAR signaling affects PKA activity in different subcellular locations for PKA-dependent phosphorylation of substrates in failing myocytes.

Recent efforts have been put forward to understand β-adrenergic signaling at the sarcolemma and the SR because of their essential roles in calcium handling and arrhythmia in cardiac diseases. By using genetically encoded biosensors, studies show that adrenergic-induced PKA activity at the SR can be selectively inhibited by chronic insulin<sup>9</sup> and the proinflammatory factor, prostaglandin E,<sup>10</sup> both of which are elevated in clinical conditions associated with heart failure. Moreover, in hypertrophic failing myocytes isolated from a transaortic constriction mouse model, the adrenergic stimulation-induced cAMP activity is reduced at the PM<sup>11</sup> and the SR,<sup>12</sup> consistent with depressed PKA phosphorylation of PLB.<sup>13</sup> In contrast, much less is known about the regulation of PKA activity and PKA phosphorylation of substrates on the myofilaments during cardiac remodeling and disease development. A disturbed PKA phosphorylation of myofilament proteins such as TnI and myosin-binding protein C alters their calcium-binding sensitivity, which directly contributes to inotropic and lusitropic dysfunction in the heart.<sup>14</sup>

Here, we develop a novel genetically encoded PKA biosensor that is anchored on the myofibrils to probe PKA activity in cardiac myocytes from a rabbit hypertrophic heart failure model.<sup>15</sup> Our data show that although the β<sub>1</sub>AR-induced PKA signal is detected at the myofilaments, the sarcolemma, and the SR in healthy myocytes, the β<sub>2</sub>AR-induced PKA signal is restricted along the sarcolemma and the SR and does not have access to the myofilaments. However, in hypertrophic failing rabbit myocytes, stimulation of β<sub>2</sub>AR promotes a strong PKA activity at the myofilaments. The emerging β<sub>2</sub>AR signal is associated with downregulation of caveolin-3 in hypertrophic failing myocytes, a key structural protein of caveolae that confines the β<sub>2</sub>AR signal.<sup>16</sup> Thus, in failing myocytes, stimulation of the β<sub>2</sub>AR promotes strong PKA activity and PKA phosphorylation of TnI. Moreover, we demonstrate that re-introduction of caveolin-3 normalizes the distribution of the

β-adrenergic signal and restores contractile response to adrenergic stimulation.

**Methods****Experimental Animals, Cardiac Myocyte Isolation, and Culture**

The animal care and experimental protocols followed US National Institutes of Health guidelines and were approved by the Institutional Animal Care and Use Committees of the University of California at Davis. Heart failure (HF) was induced in New Zealand White rabbits by combined aortic insufficiency and stenosis as previously described.<sup>15</sup>

**Fluorescence Resonance Energy Transfer Measurements**

Images were acquired using a Leica DMI3000B inverted fluorescence microscope (Leica Biosystems, Buffalo Grove, IL) with a 40× oil-immersion objective lens and a charge-coupled device camera controlled by Metafluor software (Molecular Devices, Sunnyvale, CA). Fluorescence images for fluorescence resonance energy transfer (FRET) analysis were obtained as described previously.<sup>17</sup>

**Statistical Analysis**

Statistical analysis was performed using GraphPad Prism 6 software (La Jolla, CA).

Expanded methods can be found online ([Online Data Supplement](#)).

**Results****Novel Biosensors Reveal Highly Localized β<sub>2</sub>AR-Induced PKA Activity That Does not Reach the Myofilaments in Healthy Rabbit Cardiac Myocytes**

To analyze the dynamics of PKA activity on the myofilaments, we took a novel strategy to anchor FRET-based A-kinase activity reporter 3 (AKAR3)<sup>17</sup> onto the myofilaments by linking AKAR3 to the C terminus of troponin T (myofilament-AKAR3; Figure 1A). Myofilament-AKAR3 was used together with 2 other targeted PKA biosensors developed previously: PM-AKAR3 is linked to a PM-targeting sequence from Kras and SR-AKAR3 is linked to the transmembrane domain of PLB.<sup>10,18</sup> Confocal analysis of rabbit adult cardiac myocytes shows that the biosensors display proper subcellular distribution, colocalizing with specific markers for subcellular organelles (Figure 1B). The introduction of biosensors does not affect adrenergic stimulation-induced PKA phosphorylation of endogenous TnI (Figure 1C) or PLB.<sup>10,18</sup> These data indicate that the molecular pathways are preserved on the expression of biosensors, and the targeted probes are suitable for analysis of PKA activity in the microdomains of adult cardiac myocytes.

We further characterized the AKAR3 biosensors in response to a set of incremental doses of β-adrenergic agonist isoproterenol in adult rabbit myocytes. Stimulation of myocytes with isoproterenol induces dose-dependent increases in FRET ratio of the PM-, SR-, and myofilament-anchored AKAR3 biosensors, and the maximal responses are higher at the PM than those at the SR and myofilament (Figure 1D; Online Figure I). The responses of PM-AKAR3 are also more sensitive to isoproterenol stimulation than those of SR-AKAR3 and myofilament-AKAR3 (Figure 1D and 1E; Online Figure I). These data are consistent with previous studies showing that PKA phosphorylation of substrates at the PM is

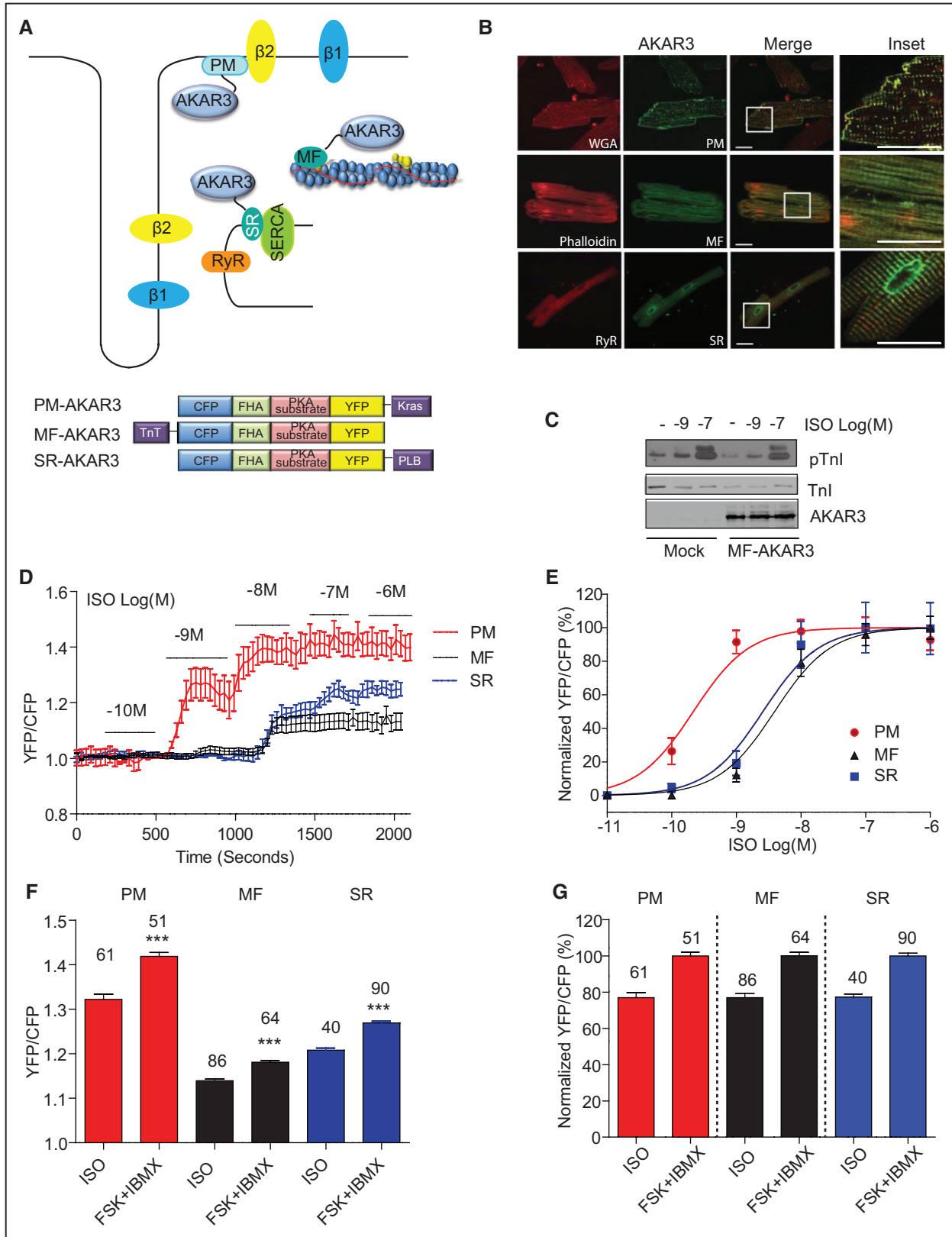


**Figure 1. Generation of cardiac myofilament-targeted fluorescence resonant energy transfer (FRET) biosensors. A,** Schematic representation of subcellular localized protein kinase A (PKA) A-kinase activity reporter 3 (AKAR3) biosensors. Yellow (YFP) and cyan (CFP) fluorescent proteins flank a PKA substrate and a forkhead-associated (FHA) domain that recognizes the phosphorylated PKA substrate. AKAR3 is linked to a Kras-derived sequence for plasma membrane (PM-AKAR3) localization, to a phospholamban (PLB)-derived sequence for sarcoplasmic reticulum (SR-AKAR3) localization, and to troponin T for myofilament (MF-AKAR3) localization. **B,** Representative confocal images of biosensor (green) expressed in young rabbit cardiac myocytes. Cells are immunostained with subcellular specific markers (red) for the SR (ryanodine receptor [RyR]), the PM (wheat germ agglutinin [WGA]), and (Continued)

**Figure 1 Continued.** the MF (phalloidin). Merge images confirm colocalization of fluorescent signals. **C**, Immunoblot analyses of PKA phosphorylation of troponin I (TnI) at serine 23/24 in response to isoproterenol (ISO) stimulation (1 or 100 nmol/L) in young rabbit myocytes infected with MF-AKAR3 probes. **D**, Young rabbit myocytes expressing PM-AKAR3, SR-AKAR3, and MF-AKAR3 are stimulated with a set of incremental doses of ISO. Time courses show AKAR3 FRET responses after stimulation with ISO. **E**, Normalized, isoproterenol-induced, dose-response curves of AKAR3 biosensors (EC<sub>50</sub> PM-AKAR3 at  $2.16 \times 10^{-10}$  mol/L, SR-AKAR3 at  $2.57 \times 10^{-9}$  mol/L, and MF-AKAR3 at  $3.89 \times 10^{-9}$  mol/L). **F**, Maximal increases in AKAR3 FRET ratio after stimulation with ISO (1  $\mu$ mol/L) or after cotreatment with forskolin (10  $\mu$ mol/L) and IBMX (3-isobutyl-1-methylxanthine; 100  $\mu$ mol/L). **G**, Normalized maximal FRET responses of individual AKAR3 biosensors against the increases induced by cotreatment with forskolin and IBMX, respectively. SERCA indicates sarco/endoplasmic reticulum Ca<sup>2+</sup>-ATPase.

more sensitive to lower doses of isoproterenol stimulation than those at the intracellular compartments.<sup>19</sup> The isoproterenol-induced maximal responses are not because of saturation of individual biosensors because cotreatment of myocytes with forskolin and IBMX (3-isobutyl-1-methylxanthine) induces higher increases in FRET ratios of biosensors than those induced by isoproterenol, respectively (Figure 1F). Notably, the isoproterenol-induced maximal responses in these localized biosensors are equivalent when normalized by those induced by cotreatment of forskolin and IBMX (Figure 1G), suggesting that these biosensors are functionally comparable in response to adrenergic stimulation in rabbit myocytes.

To analyze the alteration of local PKA dynamics at the myofilaments in failing heart, we used cardiac myocytes isolated from rabbits with hypertrophic HF induced by combined aortic insufficiency and stenosis.<sup>15</sup> Myocytes from age-matched rabbits with sham surgery (SHAM) were used as controls. In age-matched SHAM myocytes, stimulation of the  $\beta$ AR with a saturated dose of isoproterenol (100 nmol/L) leads to an increase of PKA activity, which is completely blocked by  $\beta_1$ AR selective antagonist CGP20712A but not by  $\beta_2$ AR selective antagonist ICI118551 (Figure 2A). Accordingly, stimulation of SHAM myocytes with isoproterenol significantly promotes PKA phosphorylation of TnI at serine 23/24, which is also blocked by CGP20712A but not by ICI118551 (Figure 2B). However, stimulation with isoproterenol promotes a stronger PKA activity associated with the myofilaments in failing myocytes than SHAM cells (Figure 2C and 2D). Notably, stimulation of the  $\beta_2$ AR also induces a strong increase in PKA activity in failing myocytes (Figure 2C and 2D). Consistent with the FRET measurement of PKA activity, stimulation of the  $\beta_2$ AR promotes a strong increase in PKA phosphorylation of TnI in HF myocytes but not in SHAM controls (Figure 2E). These data indicate that in HF myocytes, the  $\beta_2$ AR gains an ability to promote a strong PKA signal on the myofilaments.

### **$\beta$ AR-Induced PKA Activity Is Diminished at the SR and the PM in Failing Rabbit Myocytes**

We also examined the alteration of local PKA dynamics at the SR in failing myocytes, an important intracellular organelle that regulates calcium signaling for myocyte contraction. In SHAM myocytes, stimulation of the  $\beta$ AR promotes a significant increase in PKA activity at the SR, which is inhibited by  $\beta_1$ AR antagonist CGP20712A but not by  $\beta_2$ AR antagonist ICI118551 (Figure 3A). Consistent with the FRET-based measurement of PKA activity, stimulation of SHAM myocytes with isoproterenol promotes PKA phosphorylation of PLB at serine 16, which is completely blocked by CGP20712A but not by ICI118551 (Figure 3B). However, stimulation with isoproterenol promotes a weaker PKA activity at the SR in failing

myocytes than that in SHAM cells (Figure 3C and 3D). Further analysis reveals that the  $\beta_1$ AR-induced PKA activity at the SR is reduced, whereas the  $\beta_2$ AR-induced PKA activity at the SR is slightly increased (Figure 3C and 3D). Consistently, the adrenergic-induced PKA phosphorylation of PLB is diminished in HF myocytes compared with those in SHAM controls. In both SHAM and HF cells, the  $\beta_1$ AR acts as the primary receptor subtype in adrenergic stimulation (Figure 3E). These data indicate that in HF myocytes, the  $\beta$ AR-induced PKA activity is diminished at the SR for substrate phosphorylation.

In comparison, stimulation of  $\beta$ AR promotes a robust increase in PKA activity at the PM in SHAM myocytes, which is significantly decreased in HF myocytes (Figure 4A through 4C). Inhibition of either  $\beta_1$ AR with CGP20712A or  $\beta_2$ AR with ICI118551 attenuates PKA activity induced by isoproterenol, with a stronger inhibition by the  $\beta_1$ AR blocker CGP20712A (Figure 4B). Further analysis reveals that the reduced adrenergic response at the PM in HF myocytes is primarily because of a diminished  $\beta_1$ AR-stimulated PKA activity (Figure 4A and 4D). These data suggest that the  $\beta$ AR-induced PKA activity is diminished at the PM in failing myocytes.

### **Redistribution of Phosphodiesterase Activity Contributes to Elevated PKA Activity on the Myofilaments in Failing Heart**

Recent studies have also revealed essential roles of alteration in phosphodiesterase (PDE) expression in remodeling of adrenergic signal in HF myocytes.<sup>11,20</sup> We next studied the involvement of various cAMP PDEs on the modification of local PKA activity in HF myocytes. In SHAM myocytes, inhibition of PDE3 with cilostamide induces a strong increase in PKA activity at the myofilaments and the SR but not at the PM (Figure 5A through 5C). In comparison, inhibition of PDE4 with rolipram induces a strong response in PKA activity at the PM and, to a lesser extent, at the myofilaments and the SR (Figure 5D through 5F). Consistent with these observations, PDE3 displays colocalization with the myofilament-binding protein actin, whereas both PDE4D and PDE4B display colocalization with the PM marker caveolin-3 (Online Figure II). In HF myocytes, the myofilament-associated PDE3 activity is decreased (Figure 5A and 5G), whereas the PM-associated PDE3 activity is increased relative to SHAM controls (Figure 5C and 5I), suggesting a shifted distribution of PDE3 activity from the myofilaments to the sarcolemma. In comparison, the PM-associated PDE4 activity in HF myocytes is decreased relative to SHAM controls (Figure 5F and 5I). Meanwhile, inhibition of PDE4 induces a small increase in PKA activity at the SR in SHAM myocytes, which is enhanced in HF cells (Figure 5E and 5H). However, the SR-associated PDE3 activity is not significantly altered in HF cells (Figure 5B and 5H). In addition, inhibition



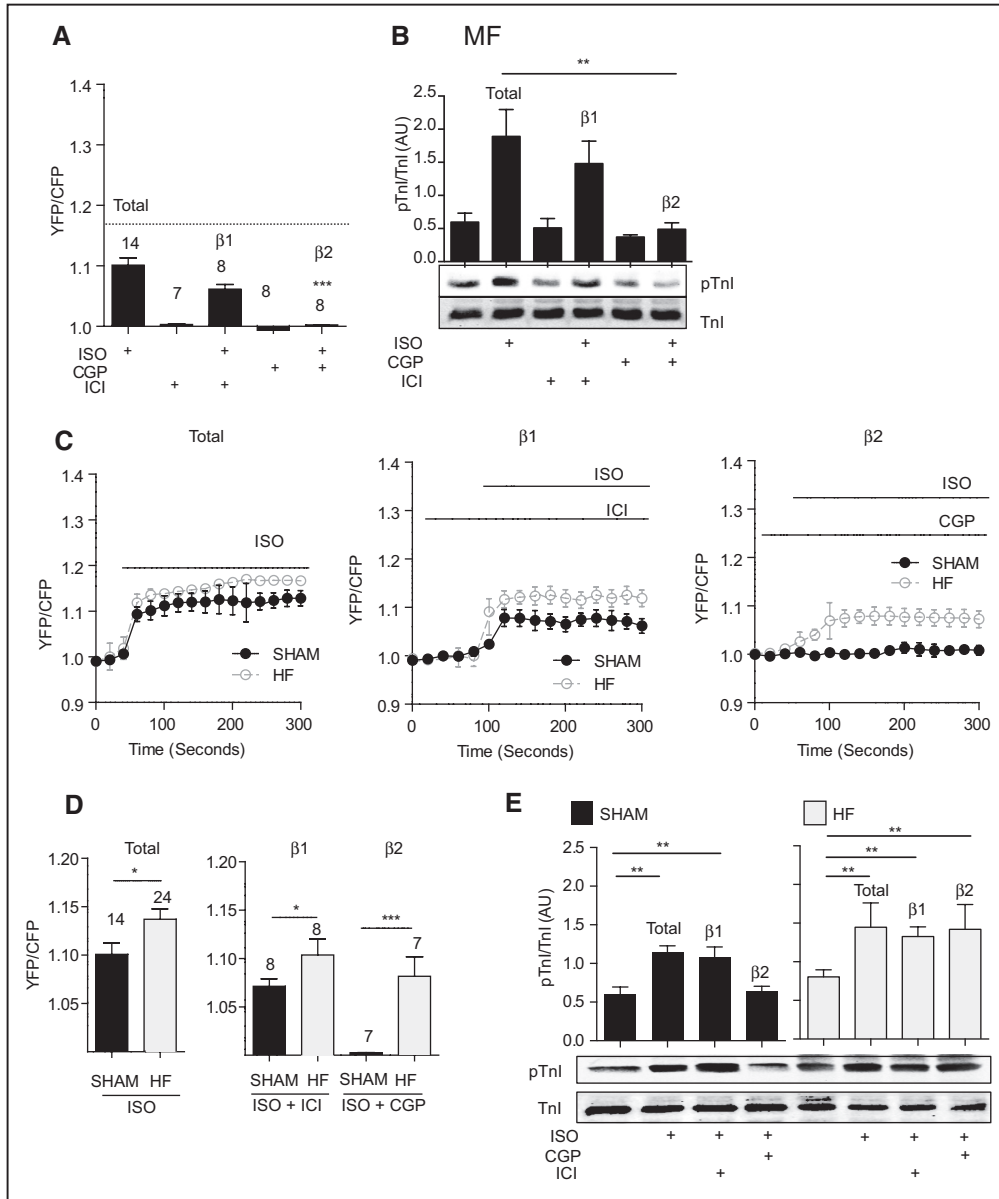


**Figure 2. A highly localized  $\beta_2$  adrenergic receptor ( $\beta_2$ AR) signal is not accessible to the myofilaments (MF) in SHAM rabbit cardiac myocytes.** **A**, SHAM rabbit cardiac myocytes expressing MF-AKAR3 are stimulated with 100 nmol/L ISO (total), or in the presence of 100 nmol/L  $\beta_1$ AR blocker ICI118551 ( $\beta_1$ AR) or 300 nmol/L of the  $\beta_1$ AR blocker CGP20712A ( $\beta_2$ AR). The maximal increases in MF-AKAR3 are plotted in bar graph. The dash line indicates the maximal increases induced by forskolin (10  $\mu$ mol/L) and IBMX (3-isobutyl-1-methylxanthine; 100  $\mu$ mol/L). \*\*\* $P$ <0.01 by 1-way ANOVA followed by post hoc Bonferroni test. **B**, Stimulation of SHAM cardiac myocytes with isoproterenol (ISO) in the presence of CGP20712A or ICI118551 for 5 minutes. The PKA phosphorylation of troponin I (TnI) at Ser 23/24 is detected in Western blot, and the increases in phosphorylation of TnI are plotted in bar graph. N=6, \*\* $P$ <0.01 by 1-way ANOVA followed by post hoc Bonferroni test. **C**, Time courses of fluorescence resonant energy transfer (FRET) responses are from SHAM and heart failure (HF) cardiac myocytes expressing MF-A-kinase activity reporter 3 (AKAR3) after stimulation of  $\beta$ ARs. **D**, Bar graph represents the maximal increases in MF-AKAR3 FRET ratio in **(C)**. \* $P$ <0.05 and \*\*\* $P$ <0.001 by Student *t* test. **E**, Stimulation of SHAM and HF cardiac myocytes with ISO in the presence of CGP20712A or ICI118551 for 5 min. The PKA phosphorylation of TnI at Ser 23/24 is detected in Western blot and quantified in bar graph. N=6, \*\* $P$ <0.01 by 1-way ANOVA followed by post hoc Bonferroni test.

of PDE2 with erythro-9-(2-hydroxy-3-nonyl)adenine induces a small increase in PKA activity at the PM and myofilaments in SHAM myocytes; the erythro-9-(2-hydroxy-3-nonyl)adenine-induced response is increased at the PM in HF cells, whereas the erythro-9-(2-hydroxy-3-nonyl)adenine-induced response is reduced at the myofilaments in HF cells (Online Figure III). Although the PDE2 activity at the SR is minimal in SHAM myocytes, it is increased in HF cells (Online Figure III).

Together, in healthy rabbit myocytes, the PKA activity at the PM is under predominant control of PDE4, whereas PDE3 hydrolyzes preferentially a pool of cAMP in the vicinity of the myofilaments (Figure 5). In HF rabbit myocytes, the presence of PDE4 activity at the PM is reduced, whereas the activity of PDE3 and PDE2 become more prominent. In contrast, the activity of PDE3 and PDE2 is decreased at the myofilaments (Figure 5; Online Figure III). These data

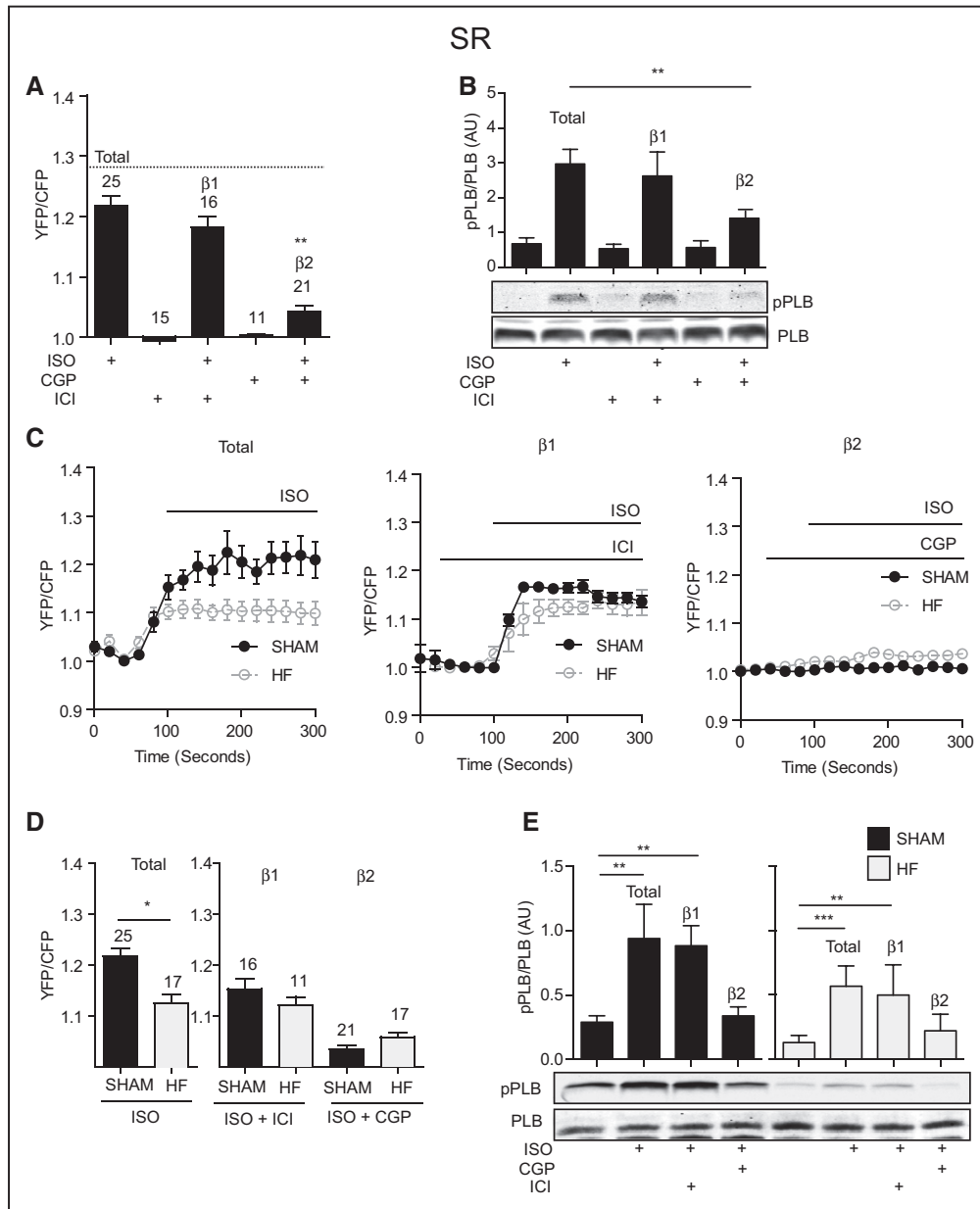


**Figure 3. Diminished  $\beta$  adrenergic receptor ( $\beta$ AR)–induced protein kinase A (PKA) activity at the sarcoplasmic reticulum (SR) in failing cardiac myocytes.** **A**, SHAM rabbit cardiac myocytes expressing SR-A-kinase activity reporter 3 (AKAR3) are stimulated with 100 nmol/L isoproterenol (ISO) (total), or in the presence of 100 nmol/L  $\beta_2$ AR blocker ICI118551 ( $\beta_1$ AR) or 300 nmol/L of the  $\beta_1$ AR blocker CGP20712A ( $\beta_2$ AR). The maximal increases in SR-AKAR3 are plotted in bar graph. The dashed line indicates the maximal increases induced by forskolin (10  $\mu$ mol/L) and IBMX (3-isobutyl-1-methylxanthine; 100  $\mu$ mol/L). \*\* $P < 0.01$  when compared with total by 1-way ANOVA followed by post hoc Bonferroni test. **B**, Stimulation of SHAM cardiac myocytes with ISO in the presence of CGP20712A or ICI118551 for 5 minutes. The PKA phosphorylation of phospholamban (PLB) at serine 16 is detected in Western blot and plotted in bar graph. N=6, \*\* $P < 0.01$  by 1-way ANOVA followed by post hoc Bonferroni test. **C**, Time courses of fluorescence resonant energy transfer (FRET) responses are from SHAM and heart failure (HF) cardiac myocytes expressing SR-AKAR3 after stimulation of  $\beta$ ARs. **D**, Bar graph represents the maximal increases in SR-AKAR3 FRET ratio in **(C)**. \* $P < 0.05$  by Student *t* test. **E**, Stimulation of SHAM and HF cardiac myocytes with ISO in the presence of CGP20712A or ICI118551 for 5 min. The PKA phosphorylation of PLB is detected in Western blot and quantified in bar graph. N=6, \*\* $P < 0.01$  and \*\*\* $P < 0.001$  by 1-way ANOVA followed by post hoc Bonferroni test.

indicate dysregulation of these hydrolytic enzymes in HF myocytes. Accordingly, Western blotting analysis shows a reduction of PDE3 and an upregulation of PDE4 expression in left ventricles after HF (Figure 6A). Moreover, PDE4 is shifted to internal compartments, whereas PDE3 is enriched at the sarcolemma region in HF myocytes relative to SHAM controls (Online Figure IV). The membrane-enriched PDE3

does not colocalize with  $\beta_2$ AR in HF myocytes (Online Figure IV). Therefore, in HF myocytes, PDEs may not be effectively coupled to adrenergic receptors. Indeed, although inhibition of PDE4 and PDE3 potentiates adrenergic stimulation–induced PKA phosphorylation of TnI in SHAM myocytes, the effects of these PDE inhibitors are diminished in the HF cells (Online Figure V).

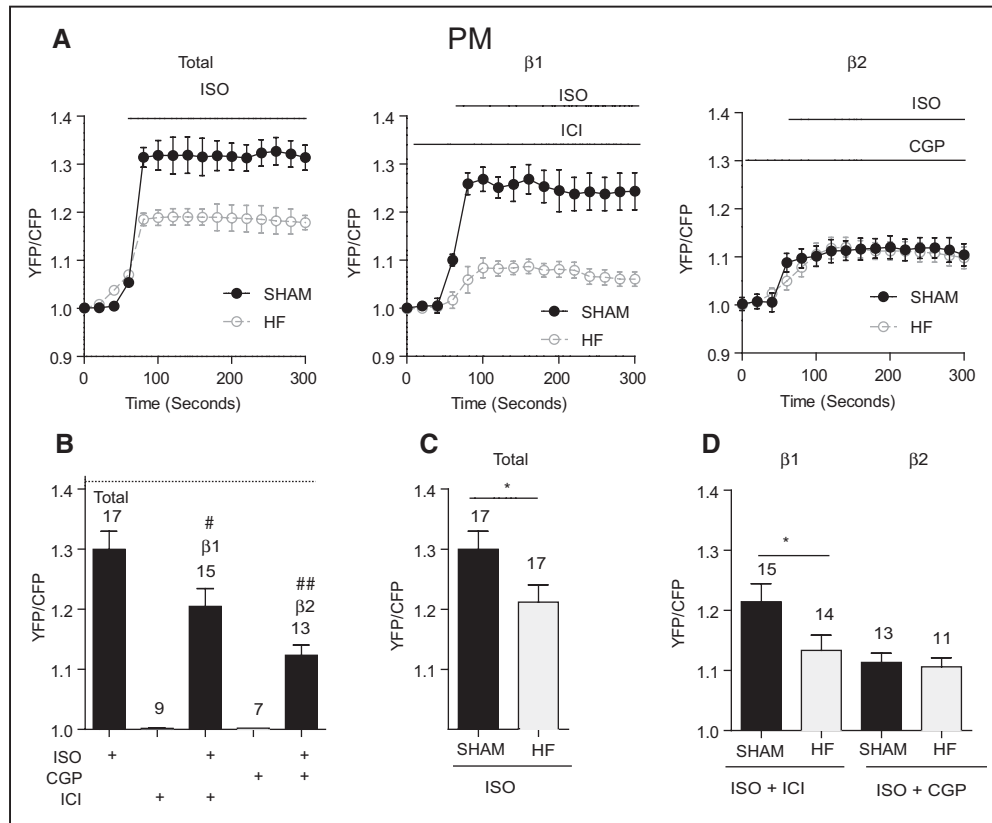


**Figure 4. Redistribution of  $\beta$  adrenergic receptor ( $\beta$ AR) subtype activity at the plasma membrane (PM) in failing cardiac myocytes.** **A**, SHAM and heart failure (HF) rabbit cardiac myocytes expressing PM-A-kinase activity reporter 3 (AKAR3) are stimulated with 100 nmol/L isoproterenol (ISO; total), in the presence of 100 nmol/L  $\beta$ 2AR blocker ICI118551 ( $\beta$ 1AR) or 300 nmol/L of the  $\beta$ 1AR blocker CGP20712A ( $\beta$ 2AR). Time courses show fluorescence resonant energy transfer (FRET) responses from SHAM and HF cardiac myocytes expressing PM-AKAR3 after stimulation of  $\beta$ ARs. **B–D**, The maximal increases in PM-AKAR3 in SHAM and HF myocytes are plotted in bar graph. In **(B)**, the dash line indicates the maximal increases induced by forskolin (10  $\mu$ mol/L) and IBMX (3-isobutyl-1-methylxanthine; 100  $\mu$ mol/L). # $P$ <0.05 and ## $P$ <0.01 by 1-way ANOVA followed by post hoc Bonferroni test. \* $P$ <0.05 by Student  $t$  test.

In a separate set of experiments, we applied PKA inhibitors in the FRET measurement to assess the baseline subcellular PKA activity in HF and SHAM myocytes (Online Figure VI). In SHAM myocytes, we detect a significant reduction of PKA activity by H89 at the myofilaments and the SR but minimal change in PKA activity at the PM (Online Figure VI). In HF myocytes, the H89-sensitive PKA activity at the PM and the SR does not change (Online Figure VI). However, the H89-sensitive PKA activity at the myofilaments is increased in HF cells, indicating an elevation of baseline PKA activity associated with myofilaments in HF myocytes (Online Figure VI).

### Reintroduction of Caveolin-3 Restores Distribution of $\beta$ AR-Induced PKA Signal, PKA Phosphorylation, and Contractility in Failing Myocytes

$\beta$ 2AR is enriched in the caveolae of cardiac myocytes, which confines the receptor action to the local PM domains. Disruption of caveolae leads to enhanced  $\beta$ 2AR stimulation of ion channels at the PM.<sup>16,21</sup> Previous studies have demonstrated that the expression of caveolin-3 is decreased in different mouse and human cardiac diseases including heart failure and hypertrophy.<sup>22–24</sup> Loss of caveolin-3 is associated with redistribution of  $\beta$ 2AR signal on the PM in failing myocytes.<sup>25</sup> Here, we reveal an 80% reduction of protein expression of

caveolin-3 in the failing rabbit myocytes. This reduction is associated with an increase of PKA phosphorylation of TnI (Figure 6A). Caveolin-3 has a scaffolding domain (C3SD) that is critical for the structure and function of caveolae. A membrane-permeable peptide corresponding to C3SD modulates  $\beta$ 2AR regulation of L-type calcium channel.<sup>21</sup> We applied the membrane-permeable C3SD peptide to healthy rabbit myocytes to examine whether inhibition of caveolin-3 promotes  $\beta$ 2AR signal to the myofilaments. Treatment with C3SD significantly enhances  $\beta$ 2AR-induced PKA activity at the myofilaments but not at the SR (Figure 6B and 6C). In contrast, a scrambled peptide does not enhance  $\beta$ 2AR-induced PKA activity at the myofilament. Consistent with the FRET-based measurement of PKA activity, C3SD significantly promotes  $\beta$ 2AR-induced PKA phosphorylation of TnI at the myofilaments (Figure 6D). These data suggest that caveolin-3 plays an essential role in preventing the  $\beta$ 2AR from signaling to the myofilaments; therefore, loss of caveolin-3 in HF myocytes may permit  $\beta$ 2AR to signal to the myofilaments to increase PKA activity and substrate phosphorylation.

We sought to restore the expression of caveolin-3 in hypertrophic failing myocytes and to evaluate  $\beta$ AR signaling and PKA activity on the myofilaments. Reintroduction of caveolin-3 partially restores the distribution of PDEs (Online

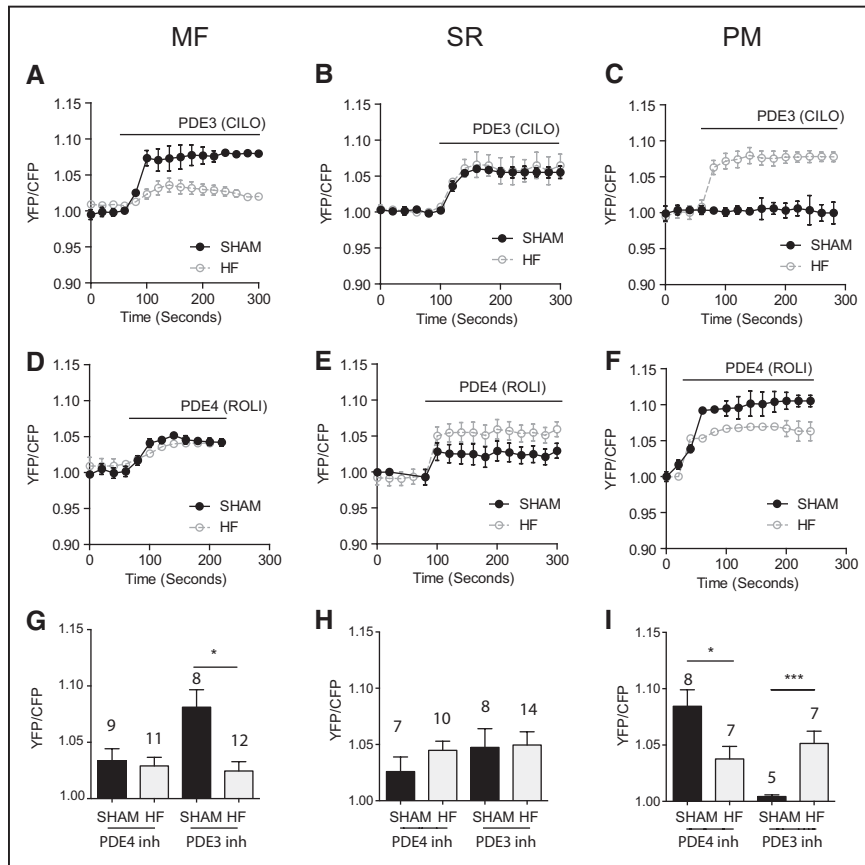


**Figure 5. Redistribution of phosphodiesterase (PDE) activity in failing cardiac myocytes.** A–F, SHAM and heart failure (HF) rabbit cardiac myocytes expressing MF-A-kinase activity reporter 3 (AKAR3), SR-AKAR3, or PM-AKAR3 are treated with 10  $\mu\text{mol/L}$  rolipram (PDE4) or 1  $\mu\text{mol/L}$  cilostamide (PDE3). Time courses of fluorescence resonant energy transfer (FRET) traces from SHAM and HF cardiac myocytes are shown. G–I, The maximal increases in AKAR3 FRET ratio in SHAM and HF myocytes are plotted in bar graph. \* $P < 0.05$  and \*\*\* $P < 0.001$  by Student *t* test.

Figure IV) and their activity in HF myocytes, including an increase in PDE4 activity at the PM and increases in PDE3 and PDE2 activity at the myofilaments (Online Figures III and VII). Moreover, reintroduction of caveolin-3 partially normalizes the distribution of  $\beta_2\text{AR}$  (Online Figure VIII) and PKA activity at the subcellular compartments, including increases in PKA activity at the PM and decreases in PKA activity at the SR and myofilaments after stimulation with isoproterenol (Figure 7A through 7C). Although the  $\beta_1\text{AR}$ -induced PKA activity is increased at the PM, the  $\beta_2\text{AR}$ -induced PKA activity is decreased throughout the myocytes. Notably, after reintroduction of caveolin-3, the  $\beta_2\text{AR}$ -induced PKA activity does not reach the myofilaments; instead, it is confined to the PM and the SR (Figure 7A through 7C). Accordingly, the phosphorylation of TnI under  $\beta_2\text{AR}$  stimulation in failing myocytes is significantly diminished after overexpression of caveolin-3 (Figure 7D). Finally, overexpression of caveolin-3 restores  $\beta$ -adrenergic-induced contractile shortening response in hypertrophic failing rabbit myocytes (Figure 7E).

## Discussion

The cardiac PKA activity is fine-tuned to ensure co-ordinated phosphorylation of substrates in different compartments for excitation–contraction coupling at baseline and after adrenergic stimulation. In this study, we have revealed a structural–functional remodeling in hypertrophic failing rabbit myocytes that links the redistribution of  $\beta\text{AR}$  signal to enhanced PKA phosphorylation of myofilament proteins (Figure 8). Although the  $\beta_2\text{AR}$ -induced signal is restricted along the sarcolemma

and the SR in healthy myocytes, an augmented  $\beta_2\text{AR}$  signal associated with loss of caveolin-3 is selectively directed to the myofilaments in hypertrophic failing cells. This augmented  $\beta_2\text{AR}$  signal, together with reduced PDE activity associated with myofibrils, promotes strong PKA activity and PKA phosphorylation of the myofilament protein TnI in hypertrophic failing myocytes. Moreover, reintroduction of caveolin-3 is able to normalize the distribution of adrenergic signaling and restores contractile response to adrenergic stimulation in hypertrophic failing rabbit myocytes.

A tonic PKA activity is maintained by adenylyl cyclase-dependent cAMP production and PDE-dependent cAMP hydrolysis.<sup>19,26</sup> Our results show that PDE4 is the major enzyme that controls local PKA activity along the sarcolemma, whereas PDE3 mediates primarily cAMP hydrolysis on the myofilaments (Figure 5). In agreement, both PDE4D and PDE4B display overlap with the membrane marker caveolin-3 (Online Figure II), consistent with a recent report showing that both enzymes have a binding motif to caveolin-3;<sup>27</sup> loss of caveolin-3 may lead to loss of PDE4 activity at the sarcolemma. In contrast, PDE3 displays a colocalization with myofibrils (Online Figure II), supporting its primary role in controlling local cAMP and PKA activity there (Figure 5). Meanwhile, we observe a high tonic PKA activity on the myofilaments, which is consistent with a relatively high PKA phosphorylation of myosin-binding protein C and TnI in healthy cardiac tissues.<sup>28</sup>

Although the PKA activity is usually depressed in the late stage of human heart failure,<sup>29,30</sup> there are reports



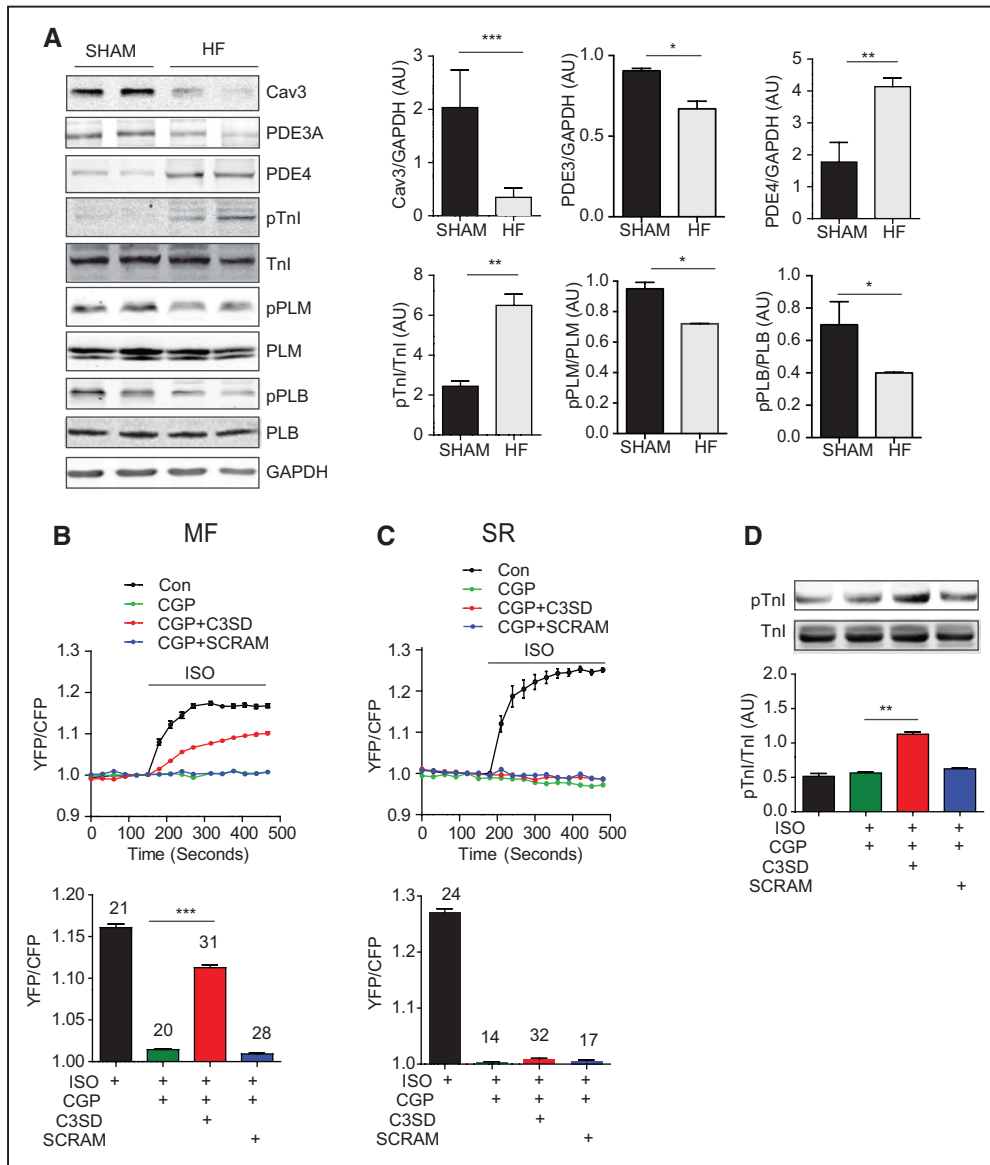


**Figure 6. Inhibition of caveolin-3 promotes adrenergic signaling on the myofilaments in heart failure (HF) cardiac myocytes.** **A**, Immunoblots show expression of caveolin-3, PDE3A, PDE4, troponin I (TnI), phospholamban (PLB), and phospholemman (PLM), as well as pTnI at serine 23/24, pPLB at serine 16, and pPLM at serine 68 in SHAM and HF heart lysates. Bar graphs represent mean±SEM. N=3; \**P*<0.05, \*\**P*<0.01, and \*\*\**P*<0.001 by Student *t* test. **B** and **C**, Healthy young rabbit myocytes expressing SR-A-kinase activity reporter 3 (AKAR3) or MF-AKAR3 are stimulated with 100 nmol/L isoproterenol (ISO) and 300 nmol/L CGP20712A after incubation with 1  $\mu$ mol/L C3SD or scrambled peptide for 1 h. Time courses of changes in AKAR3 fluorescence resonant energy transfer (FRET) ratio are shown, and the maximal increases in FRET ratio are plotted in bar graph. \*\*\**P*<0.001 by 1-way ANOVA followed by post hoc Bonferroni test. **D**, Healthy young rabbit myocytes are stimulated with 100 nmol/L ISO in the presence of 1  $\mu$ mol/L C3SD or scrambled peptide. PKA phosphorylation of troponin I at serine 23/24 is detected in Western blots and quantified in bar graph. N=3; \*\**P*<0.01 by 1-way ANOVA followed by post hoc Bonferroni test.

showing preserved or elevated PKA phosphorylation on TnI and PLB.<sup>31,32</sup> It is not completely understood how the cellular PKA activity in myocytes evolves during the course of heart failure development. Here, we observe a redistribution of PKA activity in hypertrophic failing myocytes, including an increased PKA activity at the myofilaments. In agreement, a recent report also shows that PKA phosphorylation of myofilament proteins is elevated in the spontaneous hypertensive rat model.<sup>33</sup> It is therefore possible that PKA activity is redistributed as part of the remodeling of  $\beta$ AR signaling during the compensatory stage before a general depression of PKA

activity at the late stage of heart failure. In a classic view,  $\beta$ ARs are desensitized in HF due in part to the reduced  $\beta_1$ AR density at the cell surface,<sup>34</sup> rendering the heart unable to respond to catecholamine stimulation.<sup>6</sup> However, recent progress suggests that  $\beta$ ARs can continuously signal at the cell surface<sup>7</sup> and after catecholamine-induced endocytosis.<sup>8</sup> Studies show that  $\beta$ ARs are accumulated at the endosome under chronic elevation of sympathetic activity in HF.<sup>35</sup> These  $\beta$ ARs may signal from endosomes, offering a potential mechanism on redistribution of PKA activity from the PM to the myofilaments in failing myocytes (Figures 2 and 4). Further analysis reveals

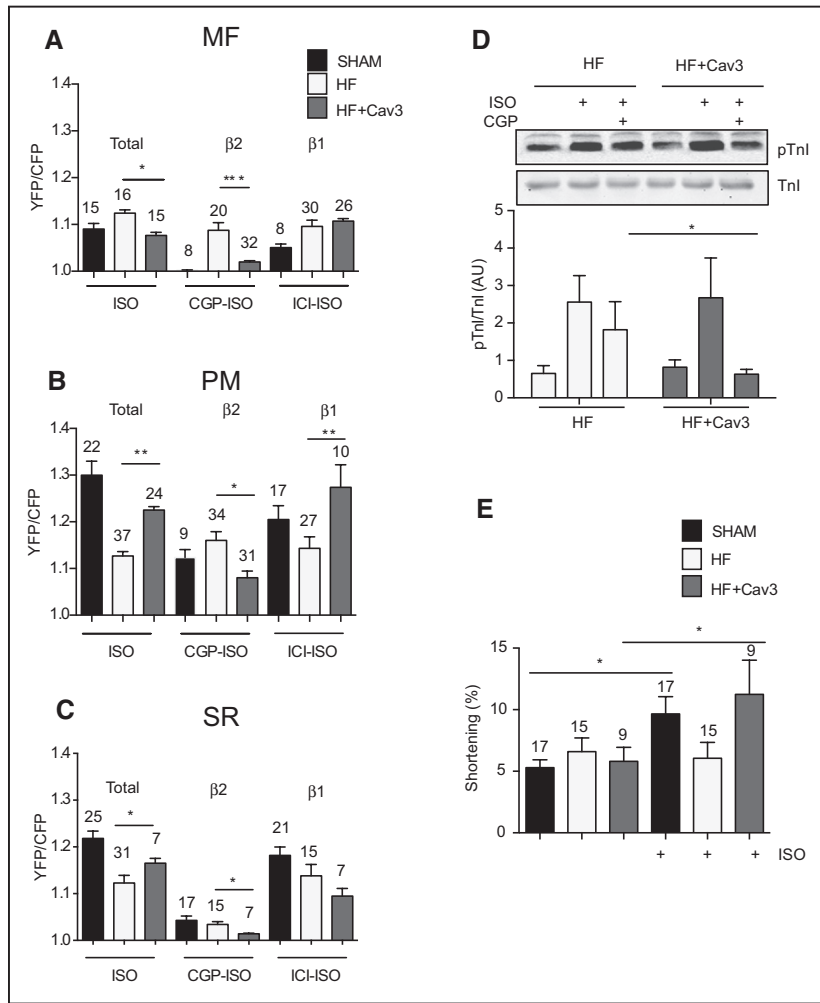


**Figure 7. Expression of caveolin-3 normalizes adrenergic signaling on the myofilaments (MFs) in heart failure (HF) cardiac myocytes. A–C,** SHAM or HF myocytes expressing MF-A-kinase activity reporter 3 (AKAR3), PM-AKAR3, or SR-AKAR3 together with caveolin-3 as indicated. Myocytes are stimulated with 100 nmol/L isoproterenol (ISO), or in the presence of 100 nmol/L ICI118551 or 300 nmol/L CGP20712A. The maximal increases in fluorescence resonant energy transfer (FRET) ratio are plotted in bar graph. \* $P < 0.05$ , \*\* $P < 0.01$ , and \*\*\* $P < 0.001$  by 1-way ANOVA followed by post hoc Bonferroni test. **D,** HF myocytes expressing caveolin-3 are stimulated with 100 nmol/L ISO in the presence of 300 nmol/L CGP20712A. PKA phosphorylation of troponin I at serine 23/24 are detected in Western blots and quantified in bar graph.  $N = 5$ ; \* $P < 0.01$  by 1-way ANOVA followed by post hoc Bonferroni test. **E,** SHAM and HF rabbit myocytes with or without expression of caveolin-3 are stimulated with ISO (100 nmol/L). Myocyte contractile shortening is plotted as bar graphs. \* $P < 0.05$  by 1-way ANOVA followed by post hoc Bonferroni test.

that the diminished  $\beta_1$ AR signaling contributes to lower PKA activity at the sarcolemma (Figure 4), which is consistent with previous observations that  $\beta_1$ AR density is downregulated in this rabbit HF model.<sup>36</sup> In comparison,  $\beta_2$ AR density is not reduced;<sup>36</sup> rather an augmented  $\beta_2$ AR signal may be preferentially directed to the myofilaments. Moreover, the shifted PKA activity can be further exacerbated by relocation of PDE3 and PDE2 activity away from the myofilaments to the sarcolemma (Figure 5; Online Figure III). Together, these observations suggest that the  $\beta$ AR signal undergoes relocation intracellularly during the development of heart failure. Further studies will likely yield novel information on  $\beta$ AR-PKA signal remodeling in subcellular compartments in models of cardiac disease, which may offer insight into cardiac hypertrophic remodeling and compensatory contractility in the heart.

Detubulation and loss of caveolae are two prominent features during cardiac structural remodeling; these alterations can in turn promote signal remodeling in cardiac myocytes. Although the  $\beta_2$ AR is confined in the tubular region in healthy myocytes, chemical disruption of caveolae with a cholesterol-depleting agent, methyl- $\beta$ -cyclodextrin, results in >60% increase in  $\beta_2$ AR-dependent PKA phosphorylation of PLB and TnI, as well as lusitropic responses in adult myocytes.<sup>37</sup> In addition, a membrane-permeable peptide representing the C3SD leads to reduction of  $\beta_2$ AR-dependent PKA phosphorylation

of L-type calcium channel at the PM.<sup>21</sup> Detubulation and loss of caveolae in hypertrophic failing myocytes isolated from a mouse model yield broad distribution of  $\beta_2$ AR signaling along the PM crest.<sup>25,37</sup> The loss of close proximity of  $\beta_2$ AR to caveolin-3-associated PDE4<sup>27</sup> can also permit a much broader reach of receptor signaling outside of the T-tubular region in failing cells.<sup>25</sup> In this study, we have observed an amplified  $\beta_2$ AR signal to the myofilaments after treatment with C3SD to promote PKA phosphorylation of TnI. Together, these observations suggest that inhibition of caveolin-3 leads to a signal shift from the PM to intracellular compartments. Moreover, we observed an amplified  $\beta_2$ AR signal associated with loss of caveolin-3 in failing rabbit myocytes, which preferentially propagates toward the myofilaments (Figures 2 and 6). These data, for the first time, link the redistribution of  $\beta_2$ AR to amplified PKA signal at the myofilaments in failing myocytes. Furthermore, reintroduction of caveolin-3 in HF myocytes can increase caveolae density,<sup>38</sup> which may facilitate the development and extension of T-tubules<sup>39</sup> and enrichment of  $\beta_2$ AR to the T-tubule (Online Figure VIII). Reintroduction of caveolin-3 may also recruit PDE4 enzymes to the proximity of the  $\beta_2$ AR local domain<sup>27</sup> (Online Figures II and IV) to confine  $\beta_2$ AR signals in local subcellular environments.<sup>25,40</sup> Consequently, reintroduction of caveolin-3 effectively prevents  $\beta_2$ AR from sending a signal to the myofilaments in rabbit failing myocytes and from promoting

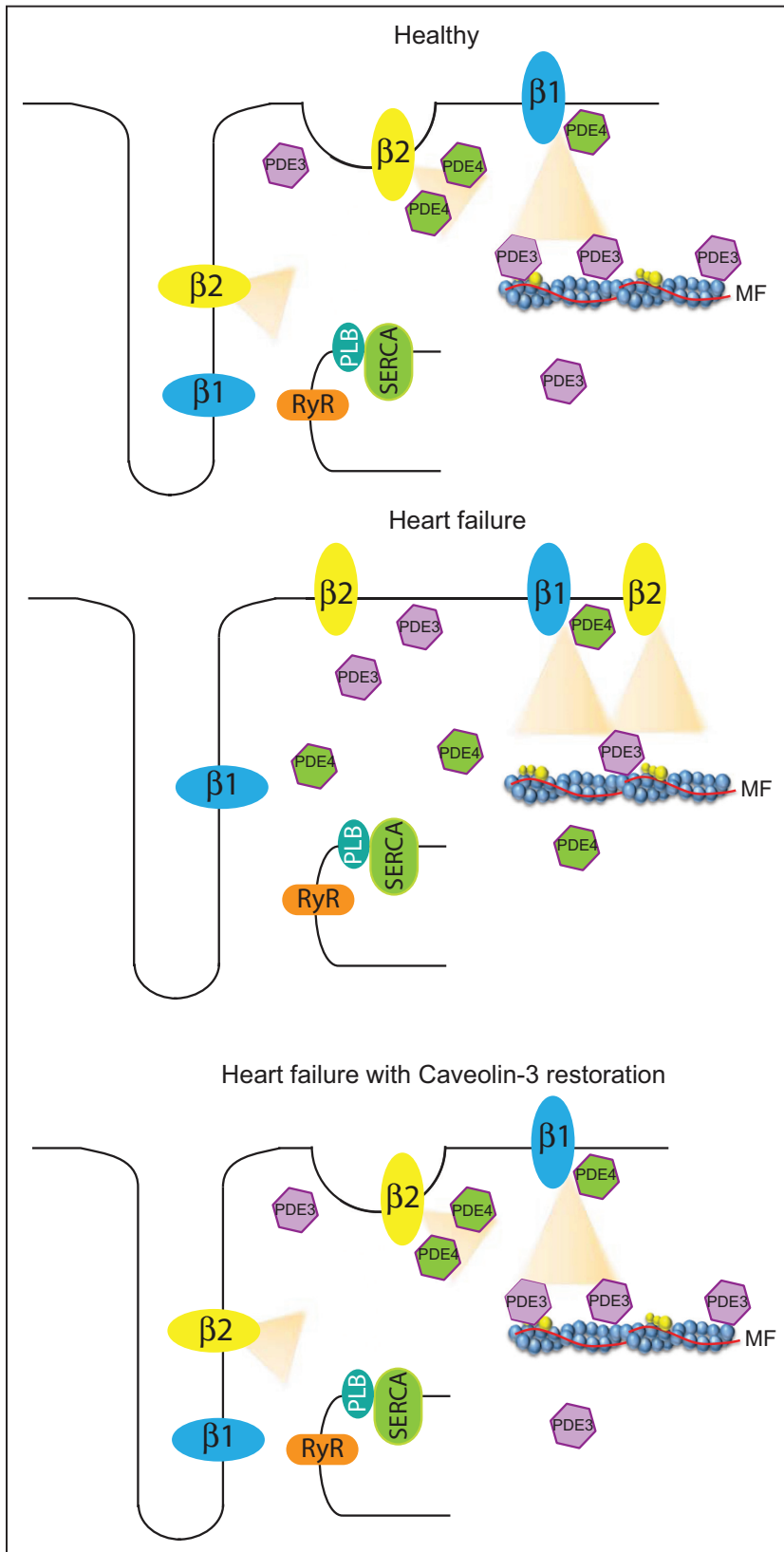


**Figure 8. Schematic models on changes of local protein kinase A (PKA) signal in failing cardiac myocytes.** In SHAM cardiac myocytes,  $\beta$ 1AR has a higher and further reaching response in all 3 subcellular compartments tested than  $\beta$ 2AR.  $\beta$ 2AR generates a highly localized response within the plasma membrane (PM) and the sarcoplasmic reticulum (SR) but does not induce any significant PKA activity on the myofilaments (MFs). PKA activity at the PM microdomain is under predominant control of PDE4, whereas PDE3 preferentially hydrolyzes a pool of cAMP in the vicinity of MFs. In HF myocytes with reduced caveolin-3, the  $\beta$  adrenergic receptor ( $\beta$ AR)-induced PKA activity at the PM and, to a lesser extent, at the SR is reduced. However, the  $\beta$ AR-induced PKA activity at the myofilament is increased due in part to augmented  $\beta$ 2AR signal and miss-localization of PDE3 away from the myofilaments. Reintroduction of caveolin-3 normalizes the distribution of  $\beta$ AR-induced PKA activity at the subcellular compartments, including increases in PKA activity at the PM and decreases in PKA activity at the MFs. In particular, the  $\beta$ 2AR-induced PKA activity is confined to the PM and the SR and does not access the myofilaments. PDE indicates phosphodiesterase; PLB, phospholamban; RyR, ryanodine receptor; and SERCA, sarco/endoplasmic reticulum  $\text{Ca}^{2+}$ -ATPase.

PKA phosphorylation of TnI (Figure 8). Moreover, reintroduction of caveolin-3 could normalize the functional relationship between  $\beta$ AR and the L-type  $\text{Ca}^{2+}$  channel at both T-tubules and caveolae.<sup>16,21</sup> As a result, the caveolin-3-expressing myocytes

become more responsive to adrenergic stimulation to enhance contractility (Figure 7). Together, these data support the notion that caveolin-3 is essential in regulation of compartmented cardiac  $\beta$ AR signaling.<sup>25,40</sup>

Together, this study reveals that structural remodeling leads to  $\beta$ AR signal remodeling in failing myocytes, which yields a decrease in PKA activity at the PM and an increase in  $\beta_2$ AR-PKA activity and phosphorylation of substrates on the myofilaments in hypertrophic rabbit hearts. Our study suggests caveolin-3 as an essential regulator of subcellular adrenergic signal at the myofilaments in myocytes.

### Acknowledgments

We thank Matt L. Stein, Linda Talken, C. Blake Nichols, Ian Palmer, Max Bergman, Lisa J. Gilardoni, Maura Ferrero, and Yan Jiang for rabbit cell isolation.

### Sources of Funding

This study is supported by NIH grant R01 HL082846 to Y.K.X., P01 HL80101 to D.B., RO1 HL091071 to H.H.P., Veteran Affairs Merit Award from the Department of Veterans Affairs BX001963 to H.H.P. and BX002900 to Y.K.X., and Italian grant FIRB 2010 RBFR10URHP to F.B. T.W. is a recipient of AHA predoctoral fellow; Q.S. is a recipient of AHA postdoctoral fellow; and Y.K.X. is an AHA-established investigator of the American Heart Association and a Shanghai Eastern Scholar.

### Disclosures

None.

### References

- Ruehr ML, Russell MA, Bond M. A-kinase anchoring protein targeting of protein kinase A in the heart. *J Mol Cell Cardiol.* 2004;37:653–665. doi: 10.1016/j.yjmcc.2004.04.017.
- Koss KL, Kranias EG. Phospholamban: a prominent regulator of myocardial contractility. *Circ Res.* 1996;79:1059–1063.
- Stelzer JE, Patel JR, Walker JW, Moss RL. Differential roles of cardiac myosin-binding protein C and cardiac troponin I in the myofibrillar force responses to protein kinase A phosphorylation. *Circ Res.* 2007;101:503–511. doi: 10.1161/CIRCRESAHA.107.153650.
- Eschenhagen T. Beta-adrenergic signaling in heart failure—adapt or die. *Nat Med.* 2008;14:485–487. doi: 10.1038/nm0508-485.
- Post SR, Hammond HK, Insel PA. Beta-adrenergic receptors and receptor signaling in heart failure. *Annu Rev Pharmacol Toxicol.* 1999;39:343–360. doi: 10.1146/annurev.pharmtox.39.1.343.
- Freeman K, Colon-Rivera C, Olsson MC, Moore RL, Weinberger HD, Grupp IL, Vikstrom KL, Iaccarino G, Koch WJ, Leinwand LA. Progression from hypertrophic to dilated cardiomyopathy in mice that express a mutant myosin transgene. *Am J Physiol Heart Circ Physiol.* 2001;280:H151–H159.
- Fu Q, Kim S, Soto D, De Arcangelis V, DiPilato L, Liu S, Xu B, Shi Q, Zhang J, Xiang YK. A long lasting  $\beta_1$  adrenergic receptor stimulation of cAMP/protein kinase A (PKA) signal in cardiac myocytes. *J Biol Chem.* 2014;289:14771–14781. doi: 10.1074/jbc.M113.542589.
- Tsvetanova NG, von Zastrow M. Spatial encoding of cyclic AMP signaling specificity by GPCR endocytosis. *Nat Chem Biol.* 2014;10:1061–1065. doi: 10.1038/nchembio.1665.
- Fu Q, Xu B, Liu Y, Parikh D, Li J, Li Y, Zhang Y, Riehle C, Zhu Y, Rawlings T, Shi Q, Clark RB, Chen X, Abel ED, Xiang YK. Insulin inhibits cardiac contractility by inducing a Gi-biased beta2-adrenergic signaling in hearts. *Diabetes.* 2014;63:2676–2689.
- Liu S, Li Y, Kim S, Fu Q, Parikh D, Sridhar B, Shi Q, Zhang X, Guan Y, Chen X, Xiang YK. Phosphodiesterases coordinate cAMP propagation induced by two stimulatory G protein-coupled receptors in hearts. *Proc Natl Acad Sci USA.* 2012;109:6578–6583. doi: 10.1073/pnas.1117862109.
- Perera RK, Nikolaev VO. Compartmentation of cAMP signalling in cardiomyocytes in health and disease. *Acta Physiol (Oxf).* 2013;207:650–662. doi: 10.1111/apha.12077.
- Sprenger JU, Perera RK, Steinbrecher JH, Lehnart SE, Maier LS, Hasenfuss G, Nikolaev VO. In vivo model with targeted cAMP biosensor reveals changes in receptor-microdomain communication in cardiac disease. *Nat Commun.* 2015;6:6965. doi: 10.1038/ncomms7965.
- El-Armouche A, Pamminger T, Ditz D, Zolk O, Eschenhagen T. Decreased protein and phosphorylation level of the protein phosphatase inhibitor-1 in failing human hearts. *Cardiovasc Res.* 2004;61:87–93.
- Messer AE, Marston SB. Investigating the role of uncoupling of troponin I phosphorylation from changes in myofibrillar Ca(2+)-sensitivity in the pathogenesis of cardiomyopathy. *Front Physiol.* 2014;5:315. doi: 10.3389/fphys.2014.00315.
- Pogwizd SM, Qi M, Yuan W, Samarel AM, Bers DM. Upregulation of Na(+)/Ca(2+) exchanger expression and function in an arrhythmogenic rabbit model of heart failure. *Circ Res.* 1999;85:1009–1019.
- Balijepalli RC, Foell JD, Hall DD, Hell JW, Kamp TJ. Localization of cardiac L-type Ca(2+) channels to a caveolar macromolecular signaling complex is required for beta(2)-adrenergic regulation. *Proc Natl Acad Sci USA.* 2006;103:7500–7505. doi: 10.1073/pnas.0503465103.
- Zhang J, Ma Y, Taylor SS, Tsien RY. Genetically encoded reporters of protein kinase A activity reveal impact of substrate tethering. *Proc Natl Acad Sci USA.* 2001;98:14997–15002. doi: 10.1073/pnas.211566798.
- Liu S, Zhang J, Xiang YK. FRET-based direct detection of dynamic protein kinase A activity on the sarcoplasmic reticulum in cardiomyocytes. *Biochem Biophys Res Commun.* 2011;404:581–586. doi: 10.1016/j.bbrc.2010.11.116.
- De Arcangelis V, Liu S, Zhang D, Soto D, Xiang YK. Equilibrium between adenylyl cyclase and phosphodiesterase patterns adrenergic agonist dose-dependent spatiotemporal cAMP/protein kinase A activities in cardiomyocytes. *Mol Pharmacol.* 2010;78:340–349. doi: 10.1124/mol.110.064444.
- Mehel H, Emons J, Vettel C, et al. Phosphodiesterase-2 is up-regulated in human failing hearts and blunts  $\beta$ -adrenergic responses in cardiomyocytes. *J Am Coll Cardiol.* 2013;62:1596–1606. doi: 10.1016/j.jacc.2013.05.057.
- Bryant S, Kimura TE, Kong CH, Watson JJ, Chase A, Suleiman MS, James AF, Orchard CH. Stimulation of ICa by basal PKA activity is facilitated by caveolin-3 in cardiac ventricular myocytes. *J Mol Cell Cardiol.* 2014;68:47–55. doi: 10.1016/j.yjmcc.2013.12.026.
- Markandeya YS, Phelan LJ, Woon MT, Keefe AM, Reynolds CR, August BK, Hacker TA, Roth DM, Patel HH, Balijepalli RC. Caveolin-3 overexpression attenuates cardiac hypertrophy via inhibition of T-type Ca2+ current modulated by protein kinase C $\alpha$  in cardiomyocytes. *J Biol Chem.* 2015;290:22085–22100. doi: 10.1074/jbc.M115.674945.
- Feiner EC, Chung P, Jasmin JF, et al. Left ventricular dysfunction in murine models of heart failure and in failing human heart is associated with a selective decrease in the expression of caveolin-3. *J Card Fail.* 2011;17:253–263. doi: 10.1016/j.cardfail.2010.10.008.
- Horikawa YT, Panneerselvam M, Kawaraguchi Y, Tsumumi YM, Ali SS, Balijepalli RC, Murray F, Head BP, Niesman IR, Rieg T, Vallon V, Insel PA, Patel HH, Roth DM. Cardiac-specific overexpression of caveolin-3 attenuates cardiac hypertrophy and increases natriuretic peptide expression and signaling. *J Am Coll Cardiol.* 2011;57:2273–2283. doi: 10.1016/j.jacc.2010.12.032.
- Wright PT, Nikolaev VO, O'Hara T, Diakonov I, Bhargava A, Tokar S, Schobesberger S, Shevchuk AI, Sikkil MB, Wilkinson R, Trayanova NA, Lyon AR, Harding SE, Gorelik J. Caveolin-3 regulates compartmentation of cardiomyocyte beta2-adrenergic receptor-mediated cAMP signaling. *J Mol Cell Cardiol.* 2014;67:38–48. doi: 10.1016/j.yjmcc.2013.12.003.
- Fu Q, Chen X, Xiang YK. Compartmentalization of  $\beta$ -adrenergic signals in cardiomyocytes. *Trends Cardiovasc Med.* 2013;23:250–256. doi: 10.1016/j.tcm.2013.02.001.
- Timofeyev V, Myers RE, Kim HJ, Woltz RL, Sirish P, Heiserman JP, Li N, Singapurli A, Tang T, Yarov-Yarovoy V, Yamoah EN, Hammond HK, Chiamvimonvat N. Adenylyl cyclase subtype-specific compartmentalization: differential regulation of L-type Ca2+ current in ventricular myocytes. *Circ Res.* 2013;112:1567–1576. doi: 10.1161/CIRCRESAHA.112.300370.
- Gresham KS, Stelzer JE. The contributions of cardiac myosin binding protein C and troponin I phosphorylation to  $\beta$ -adrenergic enhancement of in vivo cardiac function. *J Physiol.* 2016;594:669–686. doi: 10.1113/JP270959.
- van der Velden J, Narolska NA, Lamberts RR, Boontje NM, Borbély A, Zaremba R, Bronzwaer JG, Papp Z, Jaquet K, Paulus WJ, Stienen GJ. Functional effects of protein kinase C-mediated myofilament phosphorylation in human myocardium. *Cardiovasc Res.* 2006;69:876–887. doi: 10.1016/j.cardiores.2005.11.021.
- Schulz EM, Wilder T, Chowdhury SA, Sheikh HN, Wolska BM, Solaro RJ, Wiecek DF. Decreasing tropomyosin phosphorylation rescues tropomyosin-induced familial hypertrophic cardiomyopathy. *J Biol Chem.* 2013;288:28925–28935. doi: 10.1074/jbc.M113.466466.



31. Fraysse B, Weinberger F, Bardswell SC, Cuello F, Vignier N, Geertz B, Starbatty J, Krämer E, Coirault C, Eschenhagen T, Kentish JC, Avkiran M, Carrier L. Increased myofilament Ca<sup>2+</sup> sensitivity and diastolic dysfunction as early consequences of Mybpc3 mutation in heterozygous knock-in mice. *J Mol Cell Cardiol.* 2012;52:1299–1307. doi: 10.1016/j.yjmcc.2012.03.009.
32. McKee LA, Chen H, Regan JA, Behunin SM, Walker JW, Walker JS, Konhilas JP. Sexually dimorphic myofilament function and cardiac troponin I phosphospecies distribution in hypertrophic cardiomyopathy mice. *Arch Biochem Biophys.* 2013;535:39–48. doi: 10.1016/j.abb.2012.12.023.
33. Dong X, Sumandea CA, Chen YC, Garcia-Cazarin ML, Zhang J, Balke CW, Sumandea MP, Ge Y. Augmented phosphorylation of cardiac troponin I in hypertensive heart failure. *J Biol Chem.* 2012;287:848–857. doi: 10.1074/jbc.M111.293258.
34. Rockman HA, Koch WJ, Lefkowitz RJ. Seven-transmembrane-spanning receptors and heart function. *Nature.* 2002;415:206–212. doi: 10.1038/415206a.
35. Perrino C, Naga Prasad SV, Schroder JN, Hata JA, Milano C, Rockman HA. Restoration of beta-adrenergic receptor signaling and contractile function in heart failure by disruption of the betaARK1/phosphoinositide 3-kinase complex. *Circulation.* 2005;111:2579–2587. doi: 10.1161/CIRCULATIONAHA.104.508796.
36. Desantiago J, Ai X, Islam M, Acuna G, Ziolo MT, Bers DM, Pogwizd SM. Arrhythmogenic effects of beta2-adrenergic stimulation in the failing heart are attributable to enhanced sarcoplasmic reticulum Ca load. *Circ Res.* 2008;102:1389–1397. doi: 10.1161/CIRCRESAHA.107.169011.
37. Calaghan S, Kozera L, White E. Compartmentalisation of cAMP-dependent signalling by caveolae in the adult cardiac myocyte. *J Mol Cell Cardiol.* 2008;45:88–92. doi: 10.1016/j.yjmcc.2008.04.004.
38. Galbiati F, Volonte D, Chu JB, Li M, Fine SW, Fu M, Bermudez J, Pedemonte M, Weidenheim KM, Pestell RG, Minetti C, Lisanti MP. Transgenic overexpression of caveolin-3 in skeletal muscle fibers induces a Duchenne-like muscular dystrophy phenotype. *Proc Natl Acad Sci USA.* 2000;97:9689–9694. doi: 10.1073/pnas.160249097.
39. Parton RG, Way M, Zorzi N, Stang E. Caveolin-3 associates with developing T-tubules during muscle differentiation. *J Cell Biol.* 1997;136:137–154.
40. Macdougall DA, Agarwal SR, Stopford EA, Chu H, Collins JA, Longster AL, Colyer J, Harvey RD, Calaghan S. Caveolae compartmentalise  $\beta$ 2-adrenoceptor signals by curtailing cAMP production and maintaining phosphatase activity in the sarcoplasmic reticulum of the adult ventricular myocyte. *J Mol Cell Cardiol.* 2012;52:388–400. doi: 10.1016/j.yjmcc.2011.06.014.

## Novelty and Significance

### What Is Known?

- Abnormal protein kinase A phosphorylation of substrates on myofilaments directly contributes to inotropic and lusitropic dysfunction in heart failure (HF).
- Adrenergic signaling is altered in HF myocytes, including downregulation of  $\beta_1$  adrenergic receptor ( $\beta_1$ AR)-induced signals and an increase in the  $\beta_2$ AR-induced signal.

### What New Information Does This Article Contribute?

- In HF myocytes,  $\beta_1$ AR-induced signaling is selectively downregulated at the sarcolemma, whereas  $\beta_2$ AR-induced signaling gains access to myofilament.
- Reintroduction of caveolin-3 in HF myocytes prevents  $\beta_2$ ARs from sending signal to myofilaments for substrate phosphorylation.
- Reintroduction of caveolin-3 normalizes  $\beta$ AR-induced contractile responses in HF myocytes.

These studies reveal that  $\beta$ AR signaling undergoes remodeling in HF myocytes, which shifts the protein kinase A activity from the cell surface to the intracellular compartments including the sarcoplasmic reticulum and myofilaments. In particular,  $\beta_2$ AR-induced signals gain access to the myofilament, which contributes to abnormal protein kinase A phosphorylation of troponin I and contractile dysfunction. Preclinical studies to assess the effects of inhibition of  $\beta_2$ AR signal on HF are indicated.

# Circulation Research

JOURNAL OF THE AMERICAN HEART ASSOCIATION



## Genetically Encoded Biosensors Reveal PKA Hyperphosphorylation on the Myofilaments in Rabbit Heart Failure

Federica Barbagallo, Bing Xu, Gopireddy R. Reddy, Toni West, Qingtong Wang, Qin Fu, Minghui Li, Qian Shi, Kenneth S. Ginsburg, William Ferrier, Andrea M. Isidori, Fabio Naro, Hemal H. Patel, Julie Bossuyt, Donald Bers and Yang K. Xiang

*Circ Res.* 2016;119:931-943; originally published online August 30, 2016;  
doi: 10.1161/CIRCRESAHA.116.308964

*Circulation Research* is published by the American Heart Association, 7272 Greenville Avenue, Dallas, TX 75231  
Copyright © 2016 American Heart Association, Inc. All rights reserved.  
Print ISSN: 0009-7330. Online ISSN: 1524-4571

The online version of this article, along with updated information and services, is located on the World Wide Web at:

<http://circres.ahajournals.org/content/119/8/931>

Data Supplement (unedited) at:

<http://circres.ahajournals.org/content/suppl/2016/08/30/CIRCRESAHA.116.308964.DC1.html>

**Permissions:** Requests for permissions to reproduce figures, tables, or portions of articles originally published in *Circulation Research* can be obtained via RightsLink, a service of the Copyright Clearance Center, not the Editorial Office. Once the online version of the published article for which permission is being requested is located, click Request Permissions in the middle column of the Web page under Services. Further information about this process is available in the [Permissions and Rights Question and Answer](#) document.

**Reprints:** Information about reprints can be found online at:  
<http://www.lww.com/reprints>

**Subscriptions:** Information about subscribing to *Circulation Research* is online at:  
<http://circres.ahajournals.org/subscriptions/>

## **Supplement Materials.**

### **Online expanded Methods**

#### **Development of PKA FRET-based biosensor and adenovirus construction**

The regular PKA activity biosensor AKAR3<sup>1</sup> was linked to the C-terminus of cardiac troponin T (provided by Dr. Jianpin Jin, Wayne State University, OH) to generate a myofilament-anchored AKAR3, termed MF-AKAR3. The recombinant construct in pcDNA3.1 (Invitrogen, CA, USA) was verified by DNA sequencing. MF-AKAR3 cDNA was subsequently subcloned into a shuttle vector pAdTrack-CMV to generate recombinant adenovirus according to the manufacturer's instructions (Quantum Biotechnologies, Republic of South Africa). The PM-AKAR3 and SR-AKAR3 have been reported previously.<sup>2,3</sup>

#### **Experimental animals, cardiac myocyte isolation and culture**

The animal care and experimental protocols followed US National Institutes of Health guidelines and were approved by the Institutional Animal Care and Use Committees of the University of California at Davis. HF was induced in New Zealand White rabbits by combined aortic insufficiency and stenosis as previously described.<sup>4</sup> HF progression was monitored by echocardiography and myocytes were isolated 7.1±1.9 months after aortic constriction when left ventricle end-systolic dimension exceeded 1.4 cm. Briefly, rabbits were sacrificed under general anesthesia (induction with propofol 2 mg/kg followed by 2-5% isoflurane in 100% oxygen). After thoracotomy, the heart was quickly excised and rinsed in cold nominally Ca-free MEM. The right atrium was removed and the aorta opened to visualize the left coronary ostia which was then cannulated using a 4F catheter.<sup>5</sup> Perfusion of the left ventricle and left atrium was established before removal of the right ventricle free wall and application of a purse-string suture to secure the catheter in place. The remainder of the isolation procedure was then essentially as previously described.<sup>6</sup>

For myocyte cultures, cells were plated on natural mouse laminin (Life Technologies, Grand Island, NY) coated dishes in culture medium PC-1 (Lonza Walkersville, MD, USA) supplemented with 1% Penicillin-Streptomycin, PH 7.4, filtered) and infected, when specified, with PM-AKAR3, SR-AKAR3, or MF-AKAR3 biosensor together with GFP-caveolin-3 or caveolin-3 for at least 28 hours.

#### **Immunostaining**

Confocal microscopy was performed using Zeiss LSM700 microscope (Zeiss, Pleasanton, CA) equipped with a Plan-Apochromat 63X oil-immersion objective. For co-localization experiments, cells were fixed for 15 min with PFA 4%, rinsed 3 times with PBS and permeabilized with blocking solution (0.5% NP40, 2% goat serum) for 15 min. Cells were then washed and stained 2 hours with anti-RyR antibody (obtained from the DSHB, the University of Iowa, IA), anti-caveolin-3 (BD, NJ, USA #610420), anti-PDE3 (a gift from Yan Chen, University of Rochester) anti-PDE4B (a gift from Marco Conti, University of California at San Francisco) antibodies, anti-PDE4D (Ab14613) (Abcam, Cambridge, UK) followed by 1 hour of the secondary anti-mouse or anti-rabbit Alexa Fluor® 488 antibodies (A-21063 and A-11055, respectively) (Thermo Fisher,

MA, USA), or followed by Phalloidin Alexa Fluor® 568 Conjugate (A-12380) or Wheat Germ Agglutinin, Alexa Fluor® 555 Conjugate (W32464) (Thermo Fisher, MA, USA).

### **Western blotting**

Left ventricular extracts or isolated cardiac myocytes were prepared in lysis buffer (25mM Tris HCl PH 7.6, 150 mM NaCl, 1% IGEPAL, 1% Sodium deoxycholate, 0.1% SDS, 1mM EDTA) with protease and phosphatase inhibitors (Na3F 100mM, Na2VO4 1mM, glycerol 1mM, NaP2O7 2.5 mM, leupeptin 10 µg/ml, PMSF 1mM, aprotinin 10 µg/ml), and protein concentration was measured by BCA assay (Pierce, IL). Lysates were resolved by SDS-PAGE before being transferred onto a PVDF membrane (Merck Millipore Ltd. MA, USA) and incubated overnight with primary antibodies followed by IRDye 680CW or 800CW secondary antibodies and acquired with an Odyssey scanner (LI-COR Biosciences Lincoln, NE, USA). The primary antibodies used for Western blotting were as follows: anti-β<sub>2</sub>AR (sc-570) (SCBT, TX, USA), anti-PDE3A (1098-1115, NIH), anti-PDE4D (Ab14613) (Abcam, Cambridge, UK) anti-phospho-PLB (Ser16, Badrilla), anti-PLB (MA3-922) (Affinity Bioreagent, CO, USA), anti-phospho-troponin I (Ser23/24, #4004) and anti-troponin I (#4002) (Cell Signaling, MA, USA). Signal intensity was quantitated by Image Studio software version 2.1 (LI-COR Biosciences Lincoln, NE, USA).

### **Fluorescence resonance energy transfer (FRET) measurements**

Images were acquired using a Leica DMI3000B inverted fluorescence microscope (Leica Biosystems, Buffalo Grove, IL) with a 40X oil-emersion objective lens and a charge-coupled device camera controlled by Metafluor software (Molecular Devices, Sunnyvale, CA). Fluorescence images were recorded by exciting the donor fluorophore at 430-455 nm and measuring emission fluorescence with two filters (475DF40 for cyan and 535DF25 for yellow). Images were subjected to background subtraction, and were acquired every 20 seconds with exposure time of 200 ms. The donor/acceptor FRET ratio was calculated and normalized to the ratio value of baseline. The binding of cAMP to AKAR3 increases CFP/YFP FRET ratio.<sup>1</sup>

### **Adult cardiomyocyte contractility**

Fresh isolated adult cardiomyocytes were infected with GFP or GFP-caveolin-3 adenovirus for 18 hours. Cells were then placed in a dish with 3 ml beating buffer (NaCl 120 mM, KCl 5.4 mM, NaH<sub>2</sub>PO<sub>4</sub> 1.2mM, MgSO<sub>4</sub> 1.2 mM, HEPES 20mM, Glucose 5.5 mM, CaCl<sub>2</sub> 1mM, PH 7.1, filtered). Cells were paced at 1 Hz with voltage of 30 V using a SD9 stimulator (Grass Technology, Warwick, RI). Contractile shortening of myocytes were recorded on an inverted microscope (Zeiss AX10) at 20X magnification using Metamorph software (Molecular Devices, Sunnyvale, CA) with the following settings: 40 frames per second for 5 seconds, at an interval of 1 minute for a duration of 10 minutes. Isoproterenol (100 nM) was added into the dish after two movies were acquired. The percentage of myocyte fractional shortening (FS) was calculated as (maximal cell length – minimal cell length)/ maximal cell length \* 100%. Analysis was performed using Metamorph.

### **Statistical analysis**

All data were expressed as mean ± SEM. Statistical analysis was performed using GraphPad



Prism 6 software (La Jolla, CA). The sample size for each group was shown in the figure legends. The cells were from at least three sets of independent experiments. Differences between two groups were evaluated by 2-tailed Student's *t*-test; comparisons of multiple groups were performed using one-way ANOVA followed by post hoc Bonferroni test.  $p < 0.05$  was defined as statistically significant.

## Reference

1. Allen MD and Zhang J. Subcellular dynamics of protein kinase A activity visualized by FRET-based reporters. *Biochem Biophys Res Commun.* 2006;348:716-21.
2. Liu S, Li Y, Kim S, Fu Q, Parikh D, Sridhar B, Shi Q, Zhang X, Guan Y, Chen X and Xiang YK. Phosphodiesterases coordinate cAMP propagation induced by two stimulatory G protein-coupled receptors in hearts. *Proc Natl Acad Sci U S A.* 2012;109:6578-83.
3. Liu S, Zhang J and Xiang YK. FRET-based direct detection of dynamic protein kinase A activity on the sarcoplasmic reticulum in cardiomyocytes. *Biochem Biophys Res Commun.* 2011;404:581-6.
4. Pogwizd SM, Qi M, Yuan W, Samarel AM and Bers DM. Upregulation of Na(+)/Ca(2+) exchanger expression and function in an arrhythmogenic rabbit model of heart failure. *Circ Res.* 1999;85:1009-19.
5. Pogwizd SM. Nonreentrant mechanisms underlying spontaneous ventricular arrhythmias in a model of nonischemic heart failure in rabbits. *Circulation.* 1995;92:1034-48.
6. Nichols CB, Chang CW, Ferrero M, Wood BM, Stein ML, Ferguson AJ, Ha D, Rigor RR, Bossuyt S and Bossuyt J. beta-adrenergic signaling inhibits Gq-dependent protein kinase D activation by preventing protein kinase D translocation. *Circ Res.* 2014;114:1398-409.

## **Supplemental Figure legend**

**Supplemental Figure I. Dose-dependent increases in AKAR3 FRET biosensors after stimulation of  $\beta$ AR in young adult rabbit myocytes.** Rabbit myocytes expressing PM-AKAR3, SR-AKAR3, and MF-AKAR3 are stimulated with increasing doses of ISO. The maximal increases in different doses of ISO are plotted as dose response curves for individual biosensors, respectively.

**Supplemental Figure II. Distribution of PDEs in SHAM and HF rabbit cardiac myocytes** Immunostaining shows distribution between PDE4B or PDE4D (red) and caveolin-3 (green), and between PDE3A (green) and the myofilaments (phalloidin, red) in healthy, HF, or HF myocytes with caveolin-3 expression.

### **Supplemental Figure III. Redistribution of PDE2 activity in HF rabbit cardiac myocytes**

Quantification of the maximal changes in FRET ratio in SHAM and HF myocytes with or without expression of caveolin-3. Cells expressing PM-AKAR3, SR-AKAR3 or MF-AKAR are stimulated with the PDE2 selective inhibitor erythro-9-(2-hydroxy-3-nonyl)adenine (EHNA, 1  $\mu$ mol/L). \*  $p < 0.05$  and \*\*  $p < 0.01$  by one-way ANOVA followed by post hoc Bonferroni test.

**Supplemental Figure IV. Distribution of PDEs in SHAM and HF rabbit cardiac myocytes** A and B) Immunostaining shows distribution between PDE4D (red) and caveolin-3 (green), and between PDE3A (green) and the myofilaments (phalloidin, red) in SHAM, HF, or HF myocytes with caveolin-3 expression. C) HF rabbit myocytes expressing flag- $\beta_2$ AR are fixed for immunostaining to show distribution of between  $\beta_2$ AR and PDE3A or PDE4D.

**Supplemental Figure V. PDE regulates PKA-mediated phosphorylation of myofilaments in SHAM and HF rabbit cardiac myocytes.** Immunoblots show PKA phosphorylation of TnI in SHAM or HF cells after stimulation with ISO (100 nmol/L, 5 min) in the presence of PDE2 inhibitor

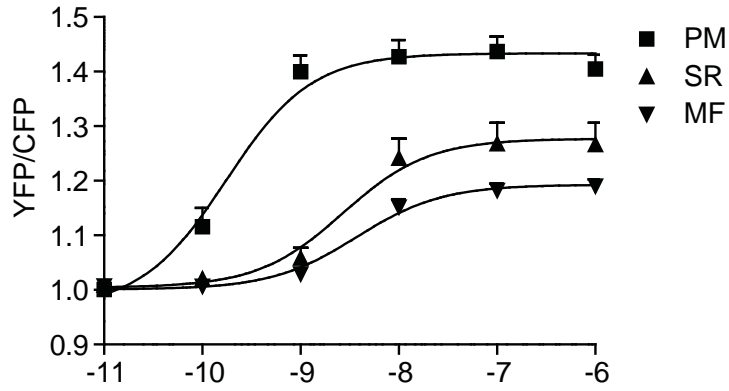
(EHNA 1  $\mu\text{mol/L}$ ), PDE3 inhibitor cilostamide (Cilo, 100 nmol/L), or PDE4 inhibitor Rolipram (Roli, 100 nmol/L). Bar graphs show mean  $\pm$  SEM, N = 4, \*  $p < 0.05$  by one-way ANOVA followed by post hoc Bonferroni test.

**Supplemental Figure VI. Detection of baseline PKA activity at the subcellular compartments in SHAM and HF rabbit myocytes.** Data shows quantification of the maximal changes in FRET ratio in SHAM and HF rabbit myocytes. A) Young adult myocytes expressing MF-AKAR3 are stimulated with ISO (100 nmol/L) in the presence of PKA inhibitor myr-PKI (10  $\mu\text{mol/L}$ ), KT5720 (10  $\mu\text{mol/L}$ ) or H89 (10  $\mu\text{mol/L}$ ). \*\*\*  $p < 0.001$  by one-way ANOVA followed by post hoc Bonferroni test. B) SHAM and HF rabbit myocytes expressing PM-AKAR3, SR-AKAR3 or MF-AKAR are treated with PKA inhibitor H89 (10  $\mu\text{mol/L}$ ). \*  $p < 0.05$  by student's *t*-test.

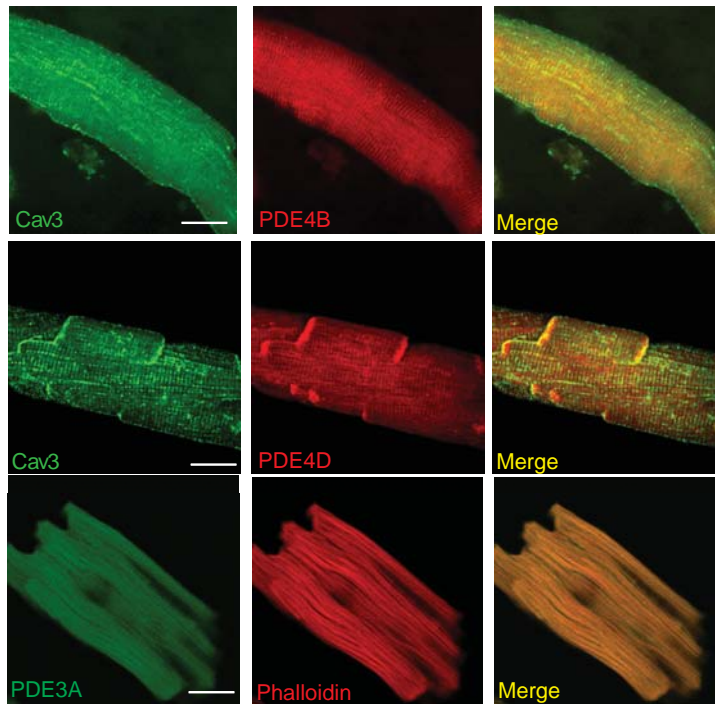
**Supplemental Figure VII. Caveolin 3 modulates subcellular distribution of PDE3 and PDE4 activity in HF rabbit cardiac myocytes.** Data shows quantification of the maximal changes in FRET ratio in SHAM myocytes and HF myocytes with or without expression of caveolin-3. Cells expressing PM-AKAR3 or MF-AKAR are treated with PDE3 selective inhibitor cilostamide (Cilo, 1  $\mu\text{mol/L}$ ) or PDE4 selective inhibitor Rolipram (Roli, 10  $\mu\text{mol/L}$ ). \*  $p < 0.05$  by student's *t*-test.

**Supplemental Figure VIII. Localization of  $\beta_2\text{AR}$  and caveolin-3 in HF rabbit cardiac myocytes.** HF rabbit myocytes expressing flag- $\beta_2\text{AR}$  alone (lower panels) or together with caveolin-3 (upper panels) are fixed for immunostaining to show distribution of  $\beta_2\text{AR}$  and caveolin-3.

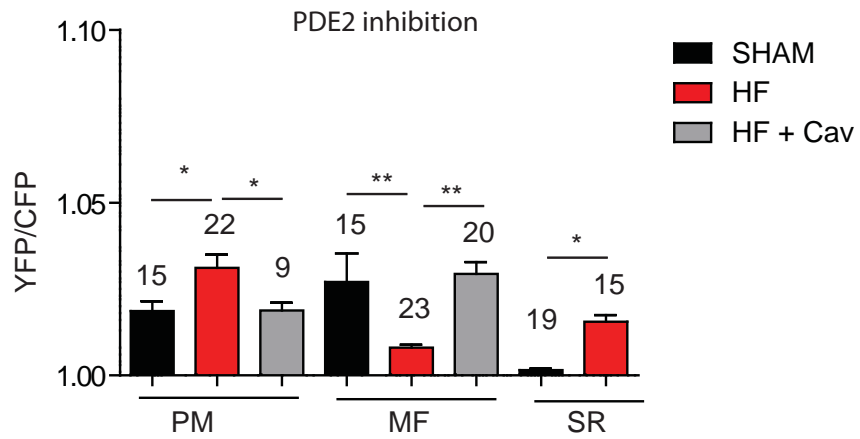
### Supplemental Figure I



### Supplemental Figure II



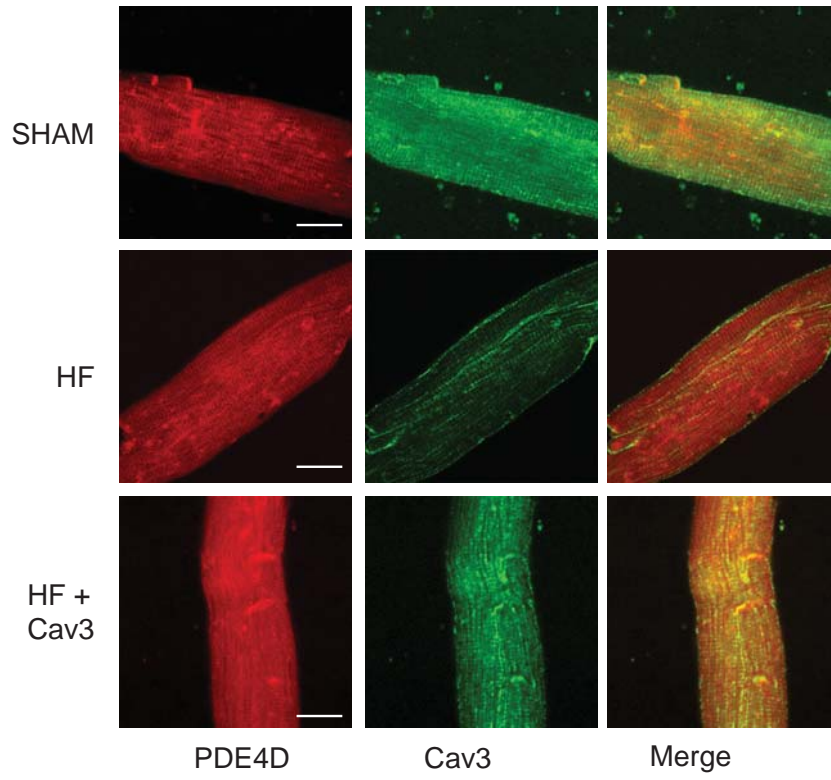
### Supplemental Figure III



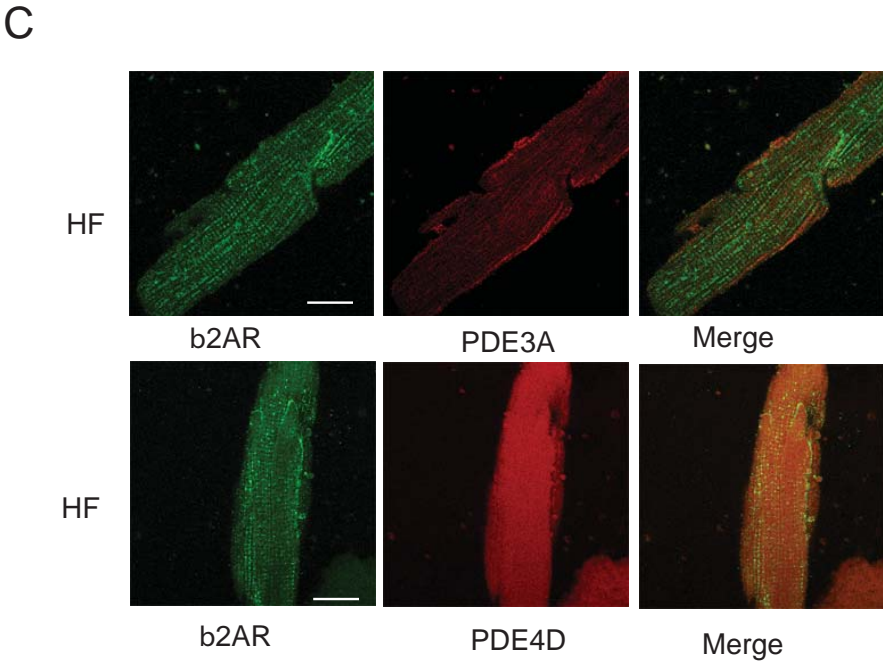
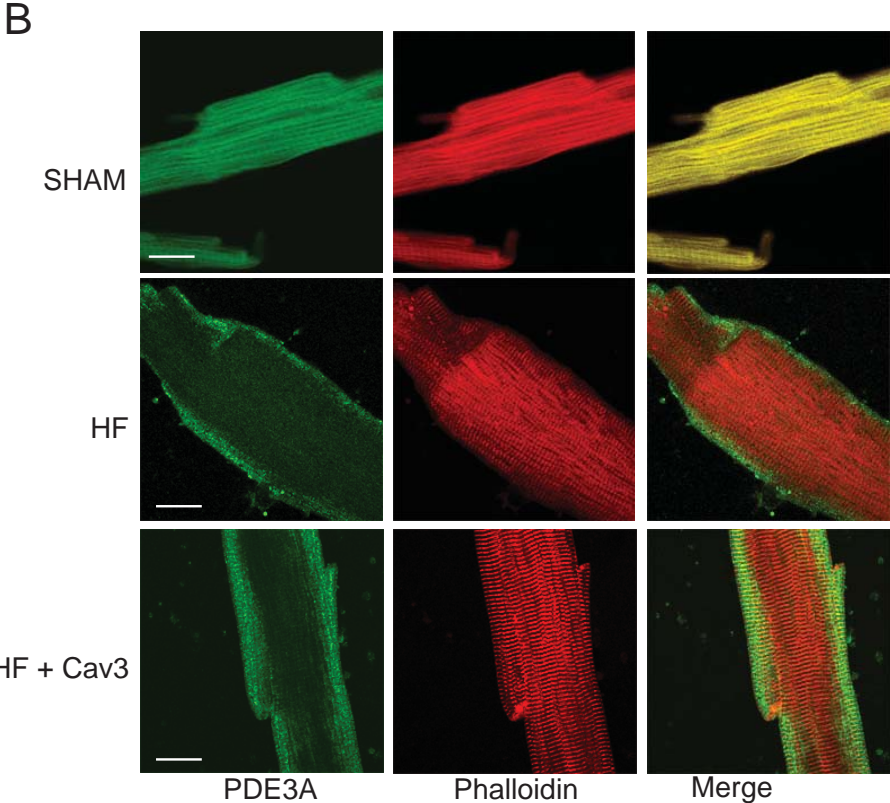


# Supplemental Figure IV

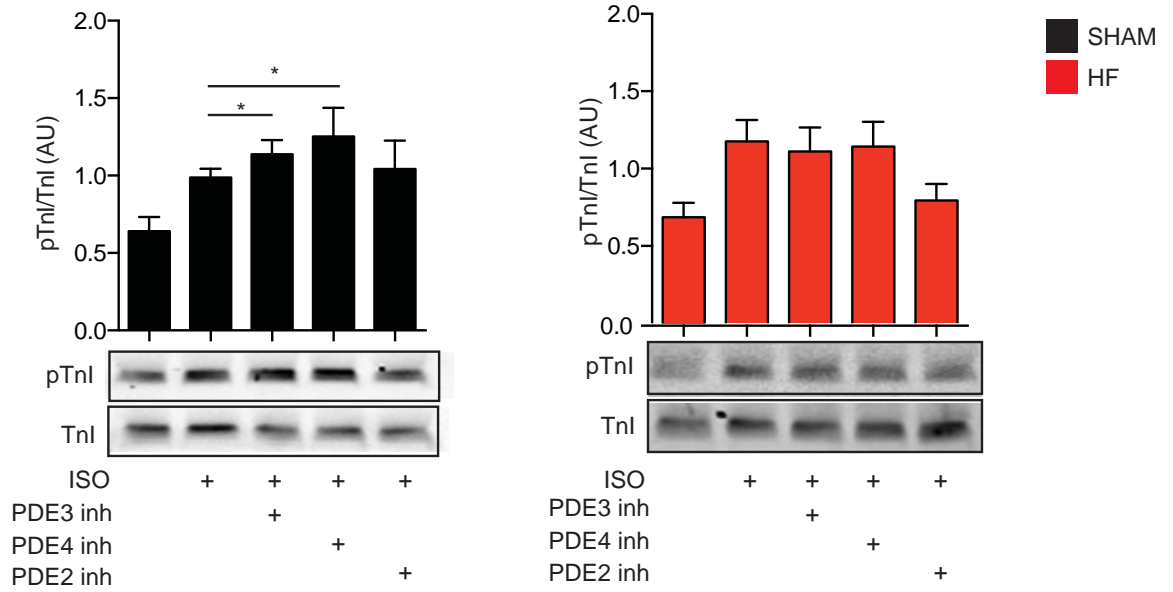
A



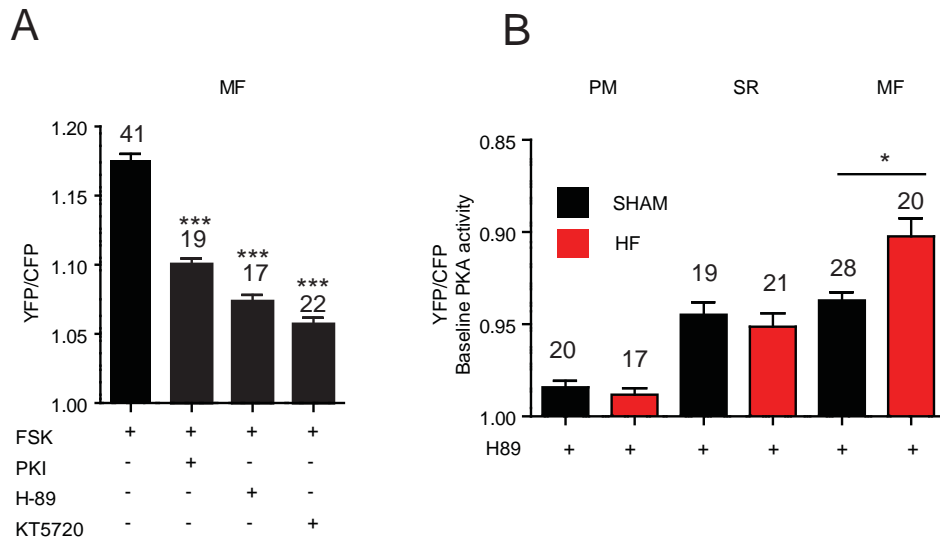
Supplemental Figure IV Continued



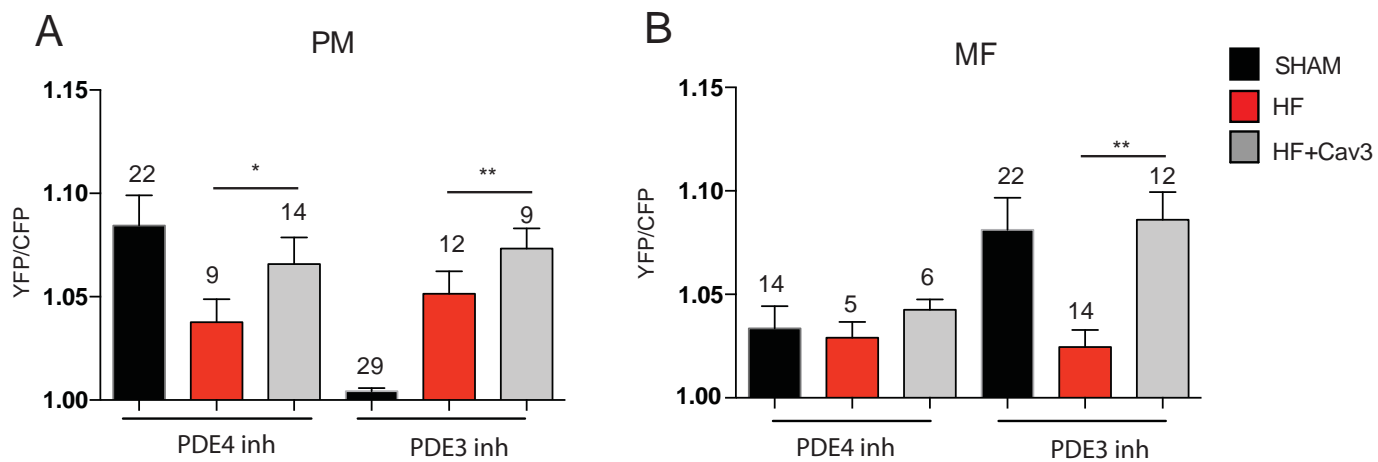
## Supplemental Figure V



## Supplemental Figure VI



## Supplemental Figure VII



## Supplemental Figure VIII

